TOMSK POLYTECHNIC UNIVERSITY ТОМСКИЙ ПОЛИТЕХНИЧЕСКИЙ УНИВЕРСИТЕТ

Министерство науки и высшего образования Российской Федерации
федеральное государственное автономное
образовательное учреждение высшего образования
«Национальный исследовательский Томский политехнический университет» (ТПУ)

Инженерная школа ядерных технологий
Направление подготовки 14.04.02 Ядерные физика и технологии
Отделение ядерно-топливного цикла

МАГИСТЕРСКАЯ ДИССЕРТАЦИЯ

Тема работы
Монте-Карло симуляция ПЭТ мелких животных

УДК 004/85:004.932

Студент

Группа	ФИО	Подпись	Дата
0АМ9М	Алексеев Никита Витальевич		

Руководитель ВКР

Должность	ФИО	Ученая степень, звание	Подпись	Дата
Директор ИШФВП	Гоголев Алексей Сергеевич	к.ф-м.н		

КОНСУЛЬТАНТЫ ПО РАЗДЕЛАМ:

По разделу «Финансовый менеджмент, ресурсоэффективность и ресурсосбережение»

Должность	ФИО	Ученая степень, звание	Подпись	Дата
Доцент ОСГН ШИП	Спицына Л.Ю.	к.ф.н.		

По разделу «Социальная ответственность»

Должность	ФИО	Ученая степень, звание	Подпись	Дата
Доцент ОЯТЦ ИЯТШ	Веригин Д.А.	к.ф-м.н		

ДОПУСТИТЬ К ЗАЩИТЕ:

Руководитель ООП	ФИО	Ученая степень, звание	Подпись	Дата
Nuclear medicine / Ядерная медицина	Верхотурова В.В.	к.и.н.		

Томск – 2021 г.

TOMSK POLYTECHNIC UNIVERSITY ТОМСКИЙ ПОЛИТЕХНИЧЕСКИЙ УНИВЕРСИТЕТ

Министерство науки и высшего образования Российской Федерации
федеральное государственное автономное
образовательное учреждение высшего образования
«Национальный исследовательский Томский политехнический университет» (ТПУ)

School of Nuclear Science & Engineering
Field of training (specialty): 14.04.02 Nuclear Science and Technology
Specialization: Nuclear medicine
Nuclear Fuel Cycle Division

MASTER THESIS

Topic of research work
Small-animal PET Monte-Carlo simulation

UDC 004/85:004.932

Student

Group	Full name	Signature	Date
0AM9M	Alekseev Nikita. Vitalevich		

Scientific supervisor

Position	Full name	Academic degree, academic rank	Signature	Date
Director of RSP	Gogolev Aleksey Sergeevich	PhD		

ADVISERS:

Section “Financial Management, Resource Efficiency and Resource Saving”

Position	Full name	Academic degree, academic rank	Signature	Date
Associate Professor	Luibov Y. Spicyna	PhD		

Section “Social Responsibility”

Position	Full name	Academic degree, academic rank	Signature	Date
Associate Professor	Dan A. Verigin	PhD		

ADMITTED TO DEFENSE:

Programme Director	Full name	Academic degree, academic rank	Signature	Date
Nuclear medicine	Vera V. Verkhoturova	PhD		

Tomsk – 2021

LEARNING OUTCOMES

Competence code	Competence name
Universal competences	
UC(U)-1	Ability to make critical analysis of problem-based situations using the systems analysis approach, and generate decisions and action plans.
UC(U)-2	Ability to run a project at all life-cycle stages.
UC(U)-3	Ability to organize and lead the teamwork and generate a team strategy to achieve the target goal.
UC(U)-4	Ability to use modern communication technologies to realize academic and professional interaction.
UC(U)-5	Ability to analyze and account for cultural diversity in the process of intercultural interaction.
UC(U)-6	Ability to set and pursue individual and professional activity priorities and ways to modify professional activity based on the self-esteem.
General professional competences	
GPC(U)-1	Ability to formulate goals and objectives of the research study, select assessment criteria, identify priorities for solving problems.
GPC(U)-2	Ability to apply modern research methods, evaluate and present the results of the performed research.
GPC(U)-3	Ability to present research outcomes in the form of articles, reports, scientific reports and presentations using computer layout systems and office software packages.
Professional competences	
PC(U)-1	Ability to maintain medical and technical documentation related to medico-physical aspects of radiation therapy, interventional radiology and radionuclide diagnostics and therapy.
PC(U)-2	Ability to ensure radiation safety of personnel, public, and the environment, to carry out monitoring of radiation exposure levels of patients, personnel, public, and the environment.
PC(U)-3	Ability to operate and maintain equipment and tools applied for the medical use of radiation.
PC(U)-4	Ability to manage the quality of physical and technical aspects within radiation therapy, diagnostics, interventional radiology and radionuclide diagnostics and therapy departments in accordance with the specific equipment requirements, regulatory requirements and staffing of a medical organization.
PC(U)-5	Ability to conduct and organize dosimetry planning, clinical dosimetry, quality assurance procedures for radiotherapy, interventional radiology, and radionuclide diagnostics and therapy.
PC(U)-6	Ability to apply knowledge of natural sciences, fundamental laws in the field of nuclear physics and technology, clinical and radiation standards, hygienic measures in nuclear medicine, which is sufficient to study issues associated with medical physics using modern equipment and information technology relying on the latest Russian and international experience.
PC(U)-7	Ability to develop reference books, tables and software containing data for clinical use in dosimetric planning of radiation therapy, radionuclide diagnostics and therapy.

Competence code	Competence name
PC(U)-8	Ability to take part in the design and physical and technical equipment development for radiation therapy, diagnostics, interventional radiology and radionuclide diagnostics and therapy, and radiation safety divisions.
PC(U)-9	Ability to conduct training sessions and develop instructional materials for the training courses within the cycle of professional training programs (bachelor degree programs).

TOMSK POLYTECHNIC UNIVERSITY ТОМСКИЙ ПОЛИТЕХНИЧЕСКИЙ УНИВЕРСИТЕТ

Министерство науки и высшего образования Российской Федерации
федеральное государственное автономное
образовательное учреждение высшего образования
«Национальный исследовательский Томский политехнический университет» (ТПУ)

School of Nuclear Science & Engineering
Field of training (specialty): 14.04.02 Nuclear Science and Technology
Specialization: Nuclear medicine
Nuclear Fuel Cycle Division

APPROVED BY:
Program Director
_____ Verkhoturova V.V.
«____» _____ 2021

ASSIGNMENT
for the Graduation Thesis completion

In the form:

Master Thesis

For a student:

Group	Full name
0AM9M	Alekseev Nikita Vitalevich

Topic of research work:

Small-animal PET Monte-Carlo simulation	
Approved by the order of the Director of School of Nuclear Science & Engineering (date, number):	№ 104-43/c dated April 14, 2021

Deadline for completion of Master Thesis:	05.06.2021

TERMS OF REFERENCE:

Initial date for research work: *(the name of the object of research or design; performance or load; mode of operation (continuous, periodic, cyclic, etc.); type of raw material or material of the product; requirements for the product, product or process; special requirements to the features of the operation of the object or product in terms of operational safety, environmental impact, energy costs; economic analysis, etc.)*	1. Spatial resolution – under 1mm. 2. Maximum number of electronic channels – 1024 3. Simulation toolkit – Geant4
List of the issues to be investigated, designed and developed *(analytical review of literary sources with the purpose to study global scientific and technological achievements in the target field, formulation of the research purpose, design, construction, determination of the procedure for research, design, and construction, discussion of the research work results, formulation of additional sections to be developed; conclusions).*	1. Analytical review of existinn small-animal PET scanners 2. Implementation of physics for PET simulation 3. Evaluation of performance charactirstics of simulated PET scanner 4. Conclusions about simulated PET data

List of graphic material *(with an exact indication of mandatory drawings)*	Presentation

Advisors to the sections of the Master Thesis
(with indication of sections)

Section	Advisor
Social responsibility	Dan A. Verigin
Financial Management, Resource Efficiency and Resource Saving	Luibov Y. Spicyna

Date of issuance of the assignment for Master Thesis completion according to the schedule	15.03.2021

Assignment issued by a scientific supervisor / advisor (if any):

Position	Full name	Academic degree, academic status	Signature	Date
Director of RSP	Gogolev Aleksey Sergeevich	PhD		

Assignment accepted for execution by a student:

Group	Full name	Signature	Date
0AM9M	Alekseev Nikita Vitalevich		

ASSIGNMENT FOR THR DIPLOMA PROJECT SECTION
«FINANCIAL MANAGEMENT, RESOURCE EFFICIENCY AND RESOURCE SAVING»

Student:

Group	Name
0AM9M	Alekseev Nikita Vitalevich

School	School of Nuclear Science & Engineering	**Department**	Division for Nuclear-Fuel Cycle
Educational level	Master	**Specialization**	14.04.02 Nuclear Science and Technology

Initial data for the section "Financial Management, Resource Efficiency and Resource Saving":	
1 The cost of scientific research resources: material, technical, energy, financial, informational and human	*Budget of research is 593401 rub.*
2 Norms and standards for spending resources	*Supervisor' salary – 72698 rub, student (researcher) salary – 148629 rub, Engineer – 1000 rub.*
3 The system of taxation used, tax rates, volumes of payments, discounts and loans	*Coefficient of incentive bonuses 30%, coefficient of incentives for the manager for conscientious work activity 25 %; contributions for social funds are 30 % totally*
Problems to research, calculate and describe:	
* *Assessment of the commercial potential of engineering solutions*	*Analysis of alternative ways of conducting research*
* *Planning of research and constructing process and making schedule for all periods of the project*	*The work consist of:* *- SWOT – analysis;* *- determination of the complexity of work.*
* *Budgeting an engineering project*	*Scientific and technical research budget consist of:* *- calculation of costs for purchasing equipment;* *- calculation of the basic and additional salary of the performers;* *- social contributions;* *- formation of the budget of costs.*
* *Calculation of resource, financial, social, budgetary efficiency of an engineering project and potential risks*	*Evaluation of efficiency is provided through:* *- integral financial indicator;* *-integral resource efficiency indicator;* *- integral efficiency indicator;* *- comparative project efficiency.*
Graphic materials	
1 Competitive power of the project *2 SWOT matrix* *3 Plan of investments. The budget for scientific and technical research* *4 Project Efficiency indicators*	

Assignment date	15.03.2021

Consultant:

Position	Name	Academic degree	Signature	Date
Associate Professor	Luibov Yurievna Spicyna	PhD		

Student:

Group	Name	Signature	Date
0AM9M	Alekseev Nikita Vitalevich		

ASSIGNMENT FOR THR DIPLOMA PROJECT SECTION
«SOCIAL RESPONSIBILITY»

Student:

Group	Name
0AM9M	Alekseev Nikita Vitalevich

School	School of Nuclear Science & Engineering	**Department**	Division for Nuclear-Fuel Cycle
Educational level	Master	**Specialization**	14.04.02 Nuclear Science and Technology

Title of graduation thesis

Small-animal PET Monte-Carlo simulation

Initial data for the section "Social responsibility":

1. Information about object of investigation (matter, material, device, algorithm, procedure, workplace) and area of its application	Positron emission tomography. Application area: Positron emission tomography of small animals
List of items to be investigated and to be developed:	
1. Legal and organizational issues to provide safety: – Special (specific for operation of objects of investigation, designed workplace) legal rules of labor legislation; – Organizational activities for layout of workplace.	– Labour code of Russian Federation #197 from 30/12/2001 GOST 12.2.032-78 SSBT – Sanitary Rules 2.2.2/2.4.1340-03. Hygienic requirements for PC and work with it
2. Work Safety: 2.1. Analysis of identified harmful and dangerous factors 2.2. Justification of measures to reduce probability of harmful and dangerous factors	– Enhanced electromagnetic radiation level – Insufficient illumination of workplace – Excessive noise – Deviation of microclimate indicators – Electric shock
3. Ecological safety:	– Indicate impact of radionuclides production on hydrosphere, atmosphere and lithosphere
4. Safety in emergency situations:	– Fire safety

Assignment date	15.03.2021

Consultant:

Position	Name	Academic degree	Signature	Date
Associate Professor	Dan Aleksandrovich Vrigin	PhD		

Student:

Group	Name	Signature	Date
0AM9M	Alekseev Nikita Vitalevich		

TOMSK POLYTECHNIC UNIVERSITY ТОМСКИЙ ПОЛИТЕХНИЧЕСКИЙ УНИВЕРСИТЕТ

Министерство науки и высшего образования Российской Федерации
федеральное государственное автономное
образовательное учреждение высшего образования
«Национальный исследовательский Томский политехнический университет» (ТПУ)

School of Nuclear Science & Engineering
Field of training (specialty): 14.04.02 Nuclear Science and Technology
Specialization: Nuclear medicine

Level of education: Master degree program
Nuclear Fuel Cycle Division
Period of completion: spring semester 2020/2021 academic year

Form of presenting the work:

Master Thesis

SCHEDULED ASSESSMENT CALENDAR
for the Master Thesis completion

Deadline for completion of Master's Graduation Thesis:	05.06.2021

Assessment date	**Title of section (module) / type of work (research)**	**Maximum score for the section (module)**
15.03.2021	*Drawing up the technical assignment*	
20.03.2021	*Calendar planning*	
30.03.2021	*Literature review*	
29.04.2021	*Choosing of scanner configuration*	
3.05.2021	*Implementation of necessary physics in Geant4*	
4.05.2021	*Simulation of detector's unit*	
5.05.2021	*Evaluation of unit's charactristics*	
6.05.2021	*Analisys of resolution properties of simulated data*	
10.05.2021	*Summarizing*	
14.05.2021	*Drawing up a final report*	
18.06.2021	*Masters's Thesis defense*	

COMPILED BY:
Scientific supervisor:

Position	**Full name**	**Academic degree, academic status**	**Signature**	**Date**
Director of RSP	Gogolev A. Sergeevich	PhD		

APPROVED BY:

Program Director	**Full name**	**Academic degree, academic status**	**Signature**	**Date**
Nuclear medicine	Vera V. Verkhoturova	PhD		

ABSTRACT

The final master's work consists of 100 pages, 16 figures, 17 tables, 20 equations, 94 sources, 4 appendixes.

Key words: positron emission tomography, small-animal, monolithic scintillator, Geant4, Monte-Carlo simulation, silicon photomultiplier.

Object of study: positron emission tomography.

Goal of work: Simulation of small-animal PET scanner.

In the work a commercially available preclinical PET scanner were observed. Based on the available parameters the PET configuration was chosen. Main features of scanner are: scintillator – LYSO; DOI estimation – monolithic scintillator; Number of channels per unit – 64; Number of all SiPMs – 1024. SiPM array pattern – checkboarded. Based on general properties the resolution characteristic of detector unit calculations show ability to estimate photon absorption position under 1 mm.

Scope of application: positron emission tomography.

Abbreviations

PET – Positron Emission Tomography

SiPM – Silicon Photomultiplier

LOR – Line of Response

FBP – Filtered-Back Projection

EM – Expectation maximization

ART – Algebraic Reconstruction Technique

MAP – Maximum a posterior

CT – Computed Tomography

MRI – Magnetic resonance imaging

TOF – Time-of-flight

FOV – Field of View

DOI – Depth-of-Interaction

PMT – Photomultiplier Tube

APD – Avalance Photodiode

Content

Introduction

Preclinical positron emission tomography (PET) is a proven non-invasive imaging method for studying disease development or progression and observing of new radiotracers and pharmaceuticals for clinical use in future. Preclinical radiological tests usually conduct for rats, mice and rarely. PET system for visualization of in this test called small-animal PET.

Due to lower size of animal compare to human images resolution should be much lower than for human studying. However, it is possible to deliver much more activity in mouse per unit volume. That is why small-animal PET system have different sizes, configuration, equipment etc.

Necessary electronic for small-animal PET increase price significant. In this work observed PET systems with ideas that allow to build cheaper configuration without dramatically loosing of resolution.

One of the ideas is to use silicone photomultipliers (SiPM) array with checkboard order cells. It means reducing number of SiPM cells in a half. However, the uniformity of resolution in such configuration should be estimated.

Second similar option is to use sparse SiPM matrix with spacing between cells. This configuration more flexible and allows to set different fill factors of SiPMs. Anyway, performance should be calculated.

On the optimization and planning stage the best option is to provide realistic simulation model and after based on it to build real detector. It is so named digital twin technology. So, in this work high mutable and flexible model of small-animal PET system is provided.

1 Literature review

1.1 PET principle

1.1.1 Radiotracers

Firstly, PET method based on radiotracers. So named tracer isotopes of element have difference in their properties (radioactivity, atomic mass) and replace original isotope in chemical compound or mixture. The behavior of the radiotracers characterizes the behavior chemical processes in body [1]. With radiotracer is also possible to track the distribution of a substance in a system of cells or tissues or describe as a tracer for flows or gases.

There are different isotopes but the most famous used in PET are: F^{18}, C^{11}, N^{13}, O^{15}. All of them are short-lived isotopes with half-time less than 2 hours. More detailed information about chemical principle of working of each tracer can be found in work [1].

Most of all PET radioisotopes are produced on cyclotron. A cyclotron consists of two hollow semicircular metal electrodes (dees) located between the poles of an electromagnet and separated by a narrow gap (Figure 1.1 [2]). An ion source (usually an electric arc in a gas) is located near the center of the dees, which serves as a generator of charged particles. At the moment of operation, the particles are pulse generated by the ion source. A filament located in an ion source creates a negative charge by attaching electrons to an atom.

When negative ions enter the vacuum chamber, they acquire energy due to the high-frequency alternating electric field induced on the dees. Ions are exposed to an electric field and a strong magnetic field generated by an electromagnet. When negative ions reach the edge of the dee and enter the gap, the radiofrequency oscillator reverses polarity on the dees and the ions are repelled as they enter the previously positively and now negatively charged dees. With each pass of the gap, the energy and radius of the orbit of the particles increase and the particles move in a spiral. When the maximum values are reached at the last turn of the spiral, a deflecting electric field is turned on, which brings the beam outward.

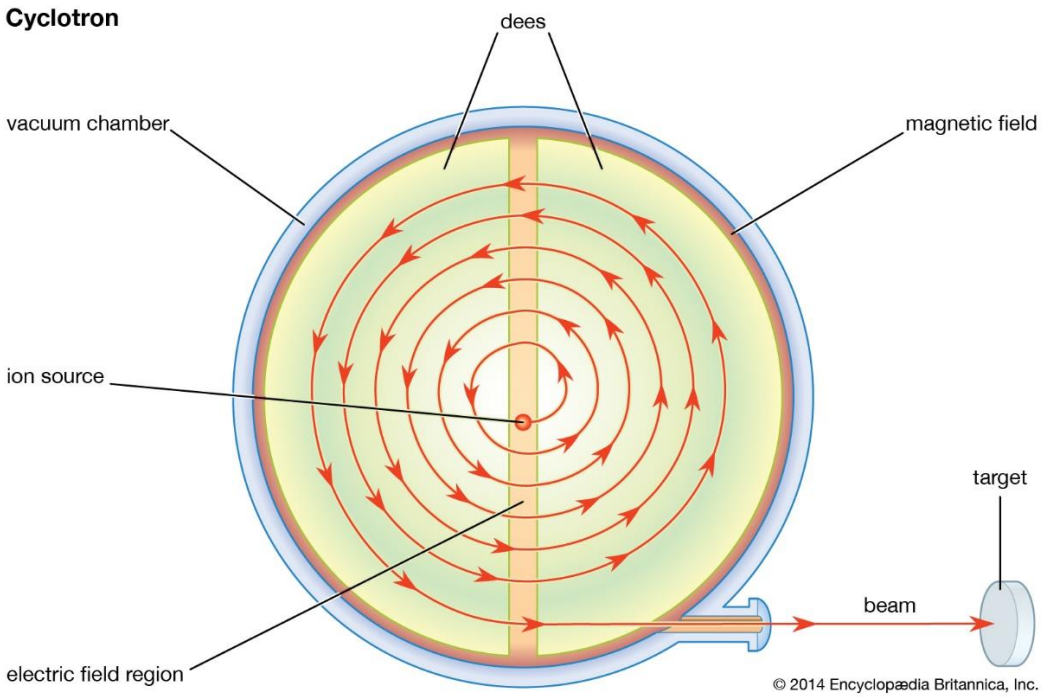

Figure 1.1 – Scheme of cyclotron

The proton beam from the cyclotron enters the target chamber and through a nuclear reaction converts the stable target material (stable chemical isotope) into a radioactive isotope [3].

The radioisotopes produced at the cyclotron are transferred to the synthesizer [4] where they are attached to the chemical compounds used in the laboratory or clinic. After the distribution in the body is wanted to be monitored. Atoms naturally occurring in organic compounds are replaced with labeled ones.

1.1.2 PET detection principle

To conduct the study, a small amount of a radioactive radionuclide is injected intravenously to the animal the radionuclide enters the cells and is distributed into them. After some time, a scanner measures its concentration in the tissues. Scanner sensitive is enough to detect even a small amount of the radioactive composition.

During the decay nucleus is overexcited by positive charge. To return on stable condition a radioactive substance positron emission occurs. A positron transfers with

some small range [5] and collides with electron of medium (usually water). In this moment positron annihilate with electron and summary energy of particles converts to two photons. Annihilation photons have energy each 511 keV and opposite directions. Therefore, after annihilation gamma particles form straight line so called line of response (LOR). Detector system register events of two photons simultaneously and when energy of inherent photons in chosen energy window. Usually for pet detectors uses scintillators and time between conversation and registration very small. Principle scheme of detection is shown in Figure 1.2 [6].

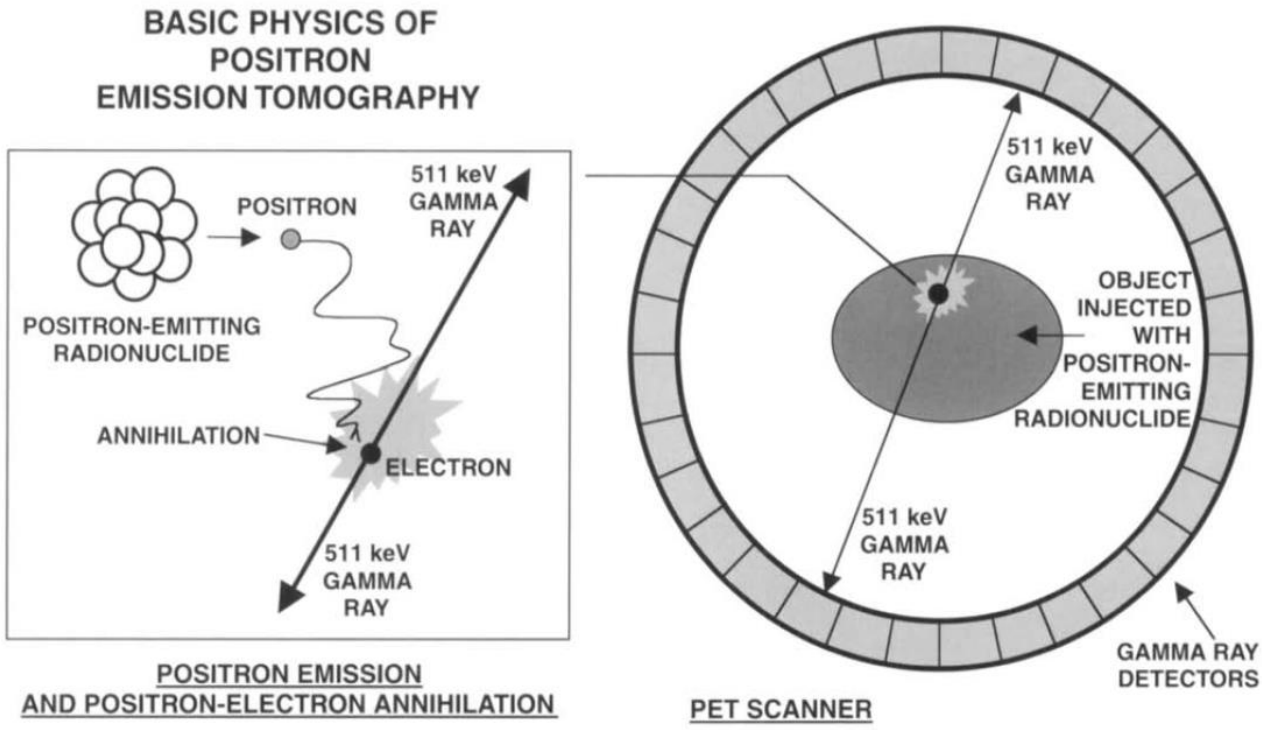

Figure 1.2 – Basic principle of PET detection

Usually scintillator with SiPM or photomultiplier tube is used for detector system. Due to much smaller size of SiPM pixel now commercial variants provide mostly SiPM variants to achieve best resolution.

1.1.3 PET reconstruction

Data acquired from scanning represents set of registered LORs. Often such data named as sinogram. LORs can be storage in different format. Import part of

visualization systems is to provide the most native and widely used representation of studying object. Reconstruction is the solution of this problem. Reconstruction is a process of transferring of raw LORs data to volume in 3D or 2D space of distribution of radioactive isotope in body.

Mathematically system of acquisition can be expressed as [7]:

$$p = H \cdot f + d, \tag{1.1}$$

where p – acquired data (set of LORs);

H – model of system, usually matrix of probabilities of voxel to produce and detect LORs;

f – unknown volume, for PET distribution of specific activity in body.

d – error of measurements, difference between “true” image and reconstructed one.

In situation when d is zero and system can be determined just through geometry problem of reconstruction could be solved analytically. Such transition from f to p from point of mathematics named as Radon transformation. Therefore, reverse transition form p to f it is inverse Random transformation [8].

Anyway, if d supposed as deterministic number or matrix of numbers the problem of reconstruction can be solved analytically. There are different methods of analytical solution. The most popular one if filtered-back projection (FBP) [9]. FBP based on back projection step where volume filled along LOR with intensity of voxels proportion to acquisition data for same value of LOR. Filtration step takes into account non-uniformity spacing of LOR in volume and allows excluding oversampling of lines problem and noises on some frequencies. In practice Ram-Lak [10, 11], Hann [12] and Sheep-Logan [13] filters. Analytical methods provide definite image, but does not include some physical specialties and dependence of noise. That is why FBP can show noisy images. However, is FBP still one of most popular methods of reconstruction due to high computation speed and low PC requirements.

More real assumption to suppose error d as stochastic value. For solution of such problem iterative methods are used [7]. There a lot of iterative methods depending

on the criteria of best image and objective function. The most popular methods are:

- Expectation maximization (EM):
  - Maximum likelihood EM (MLEM) [14, 15]
  - Ordered subset EM (OSEM) [16]
- Algebraic reconstruction technique (ART)
  - ART [17, 18]
  - Simultaneous ART (SART) [19, 20]
- Bayesian reconstruction
  - Maximum a posteriori (MAP) [21, 22]
  - Ordered subsets maximum a posteriori using one step late (OSMAPOSL) [23, 24]

Iterative algorithms allows to include noise in processing and also to provide more real model and physics properties. On the other hand, computation time could be really huge and significantly greater the FBP reconstruction time.

Often PET is combined with computed tomography (CT) or magnetic resonance imaging (MRI) there are different methods of combing results and introduce corrections such as: attenuation [25], scatter [26, 27], random [28], detector efficiency [29, 30], dead time [31].

Also modern equipment allows to use time-of-flight (TOF) technique [32, 33], but for small-animal this approach is not applicable due to sizes [34].

1.2 Existing small-animal PET scanners

There are a lot of varies of small-animal PET systems. Also papers often describe hypothetical expensive options that now unavailable for real commercial scanners. Therefore, only real commercial systems were observed.

To understand general orders of need to define comparable parameters of system.

Firstly, spatial resolution as observed option were chosen. Spatial resolution

shows the minimal distance that scanner can differentiate. Due to small size of animal's organs this parameter has high importance in visualization.

Secondly, sensitivity was observed. It describe ability to detect photons. Usually sensitivity measured in counts per unit time per unit activity. Also can be measured absolute sensitivity in percentages – ratio of emitted photons and detected one.

It is worth noting spatial resolution and sensitivity depends on location in volume and studying object. However, most of existing systems provide tests with similar phantoms and with same standard NEMA NU 4-2008 [35] [36]. So in general it is possible to provide some comparison.

Thirdly, field of view (FOV) should be included in metrics. FOV limits the size of studying object and obliviously manufactures tries to make FOV as much as possible. However, increasing of FOV increasing the cost of scanner and usually FOV has same orders as group of studying objects.

Due to big number of combined scanners with CT or MRI it is hard to find clear PET systems. As project assumes integrations with CT the PET configurations with MRI were not included.

In works [37, 38] there are observation of commercial preclinical PETs with describing. Also in work [39] comprehensive table of performance of huge amount of small-animal PETS is provided. The table is shown in Appendix A and all data sheets and other performance information of scanners is provided in this work.

Average spatial resolution through all scanners is 1.52 mm. The best value 0.89 mm is provided by Albira Si scanner by Bruker company [40]. It worth nothing Bruker scanner uses monolithic crystal of LYSO that allows to use depth-of-interaction (DOI) approach and improve determination of LORs and as a consequence the resolution. Also scanner G8 by Sofie [41] has a submillimeter resolution. But in open access a little amount of information about configuration of G8 can be found. Also it is possible to observe that for good resolutions uses iterative reconstruction methods mostly [39].

Average absolute sensitivity is about 5 %. But there are scanners with relatively huge sensitivity such as: PETBox4 by UCLA [42] (18.1 %), G8 by Sofie [41] (17.8),

β-cubes by Molecubes [43]. In the most of situations high sensitivity reaches by increasing of solid angle from point of geometry, Also or high sensitivity can be used scintillator with high stopping power and/or with high thickness [39].

On of the important properties is energy resolution. Energy resolutions defines ability to differentiate photons by energy. Average resolution through scanners is 18 %. The best value has scanners: LFER 150 by Mediso [44], The worst results have scanners: Argus by Sedecal [36] (26 %), ClearPET by Raytest GmbH [45] (25 %), LabPET12 by Gamma Medica [46] (20 %). Main parameters influenced on energy are: energy resolution of scintillator, reflectivity of surfaces, geometry and electronic photon detection efficiency (PDE).

Average transaxial FOV is around 101 mm. The biggest transaxial FOV is observed with LFER 150 by Mediso [44] (200 mm) and the smallest one with PETBox4 by UCLA [42] (45 mm). Average axial FOV is around 91 mm. The biggest axial FOV is observed with ClirvivoPET by Shimadzu [47] (151 mm) and the smallest one with VrPET by Sedecal [48] (45.6 mm) and VECTor by MILabs [49] (36 mm). In general the axial FOV is slightly lower then transaxial FOV. However, increasing of FOV increase cost of system, so FOV sizes depends significantly on required sizes of object and preferences of customers.

Below are different technical solution observed.

1.2.1 Scintillator material

PET imaging requires some properties from candidate to scintillator in detection system [50]. First off all, scintillator should have high stopping power due to high energy of photons. Higher stopping power means lower thickness of scintillator that reduce parallax effect and increase sensitivity. Secondly, light yield takes part in energy resolution and increasing of sensitivity of system. As PET uses coincidence principle useful events are important for detection. And finally, decay time is considered in scintillator choose. As activity of radioisotope could be high it is necessary to avoid dead time. In addition, spectrum emission and other parameter

should are play role with observing the detection system as an whole with photomultiplier tube (PMT) or SiPM.

BGO [51] is one of the very first scintillation materials that have been used in PET scanners. It has high stopping power and density, which allows increasing rate of counted photons. On the other hand, light yield and decay time are small enough that limits the approaches for high-resolution PET systems. Now mainly, BGO scintillator used for low-cost scanners [52].

One of the popular scintillators meeting the requirements are LYSO [53, 54] and older version LSO [54]. Lutetium scintillator have great light yield (≈ 32 photons per keV) has the same stopping power as BGO. LYSO is improved version of LSO from point of decay time (36 ns vs 40 ns) and light yield (33 photon/keV vs 26 photons/keV).

GSO [55] has great decay time and required stopping power, but small light yield compare to LYSO (7.6 photons/keV). Also GSO does not contain any radioisotopes. There are approaches shows ability of applying of GSO scintillators [56, 57].

Others scintillator used much lower but it worth nothing implementation of MLS [58] and LuYAP [59] in PET.

Table [58] with most common scintillator properties is presented below.

Table 1.1 – Main properties of commonly used PET scintillators.

	LSO	LYSO	MLS	GSO	BGO	CWO	LGSO
Light yield, ph/keV	31.00	33.20	23.56	7.60	8.5	27.3	23.56
Peak emission, nm	420	420	420	430	480	475	425
Decay time, ns	40-47	36	36-39	30-60	300	14500	40
Refractive index	1.82	1.81	18.83	1.85	2.15	2.20	1.81
Density, g/cm^3	7.4	7.1	7.3	6.71	7.13	7.9	6.5

1.2.2 PET detectors electronic

The light from scintillator should be collected with some electronic. In general, there are options such as: PMT, position sensitive PMT (PSPMT), multichannel PMT

(MCPMT), avalanche photodiode (APD) and SiPM methods [39, 60].

Most primitive PMT is works based on amplification of photoelectrons created from bombarding of photocathode by optical photons. In modern state-of-art scanners PMT is not used due to sizes of tube. With PMT's dimensions is impossible to get high resolution. Classic PET configurations use pixelated scintillator array coupled to PMT [61].

MCPMT [62] is improved version of PMT from point of gain effect. MCPMT uses micro channels coated by dynode material. Secondary electrons occurs from coating. Such configuration improve time resolution of electronic [60].

MSPMT [63] configuration distinct from MCPMT replacing single with array of small anodes (multiple anode). Such change allows to define location of inherent light. Such electronic increase resolution of system, but average cost also increased [60].

APD are highly sensitive semiconductor devices that convert light into an electrical signal due to the photoelectric effect. They can be considered as photodetectors providing internal amplification through the avalanche multiplication effect [60]. Some approaches demonstrate ability of usage for high-resolution PET as cost-efficiency [64, 65]. APD has great time and quantum efficiency performance [66].

SiPM solution combines advantages of PMT and APD [66]. SiPM has high gain and time resolution and small sizes. Hovewer, cost of such technology now not allows to use it everywhere. SiPM is solid photodetector contained bunch of small integrated single-photon avalanche diodes (microcells) [67]. There are two types of SiPMs such as: analog SiPM (a-SiPM) and digital SiPM (d-SiPM). a-SiPM contains independent cells, but connected to a common readout electronic. Such configuration have great sensitivity and detection efficiency, but it is impossible to count photons separately. d-SiPm has independent cells with independent corresponding electronic and readout. Such sensor allows to get more full information about light pulse. Consequently, d-SiPMs have high single photon sensitivity.

For small-animal PET system mainly SiPM and APD are used [39].

1.2.3 Geometry configurations

Usually PET systems represented like system of detector plates which forms ring configuration. Examples of small-animal PET configurations are shown in Figure 1.3 [68]. The geometry configuration mainly depends on required FOV or FOV's ratio and technology of detector's plates. Obliviously more FOV system costs more.

It worth nothing that older scanners give possibility to image bigger animal like monkeys so usually TFOV was big enough. Now state-of-art scanner orient on proceeding mice or rats. That is why never systems have bigger AFOV and relatively small TFOV (ring diameter).

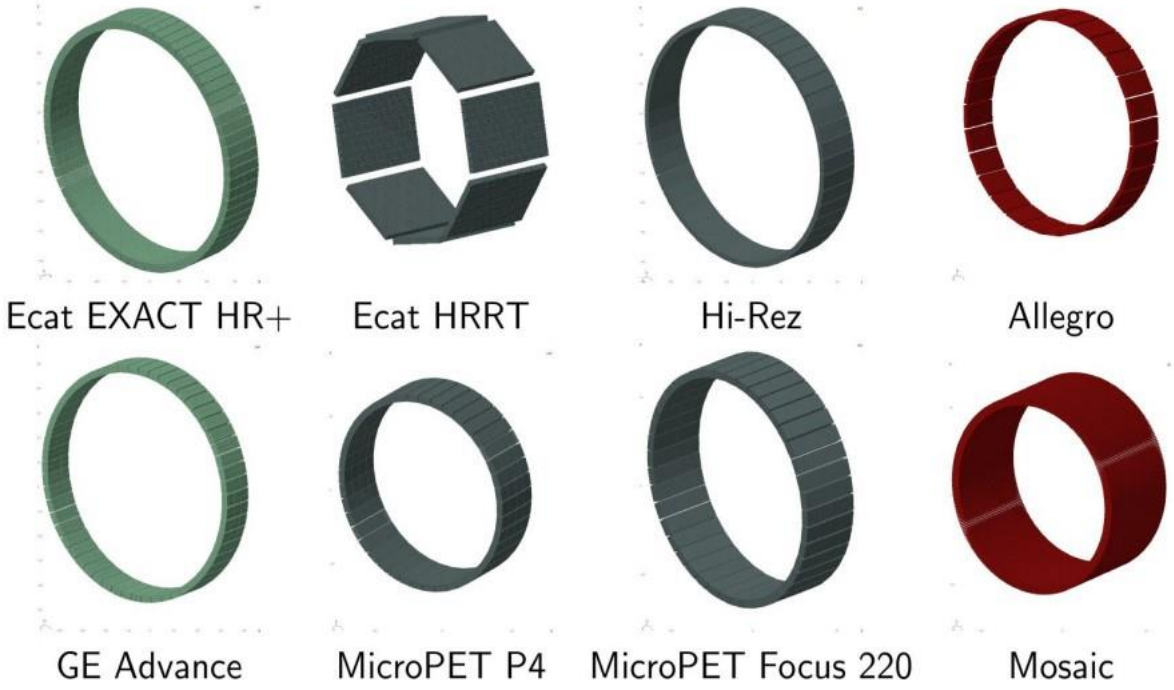

Figure 1.3 – PET geometry examples

1.2.4 Spatial resolution design considerations

Spatial resolution mainly depends on minimal size of sensitive elements. Also Geometry, configuration and range of positron are factors of spatial resolution.

Obliviously spatial resolution from point of detection system depends on ability to define LOR as close to truth as possible. Therefore, resolution of determination of

absortion point of 511 keV photons directly influenced on LOR evaluation. As was stated parallel coordinates of photon absorption to sensors plate or cells could be achieved by d-SiPM or pixelated scintillators. But due to non-zero thickness of scintillator the depth-of-interaction (DOI) is unknown from SiPM output information. In situation, when DOI considered as not detected means DOI varies from 0 to thickness of scintillator. Such uncertainty increase area of possible LOR detection. This problem is named parallax effect. In Figure 1.4 the explanation of parallax effect is shown [69].

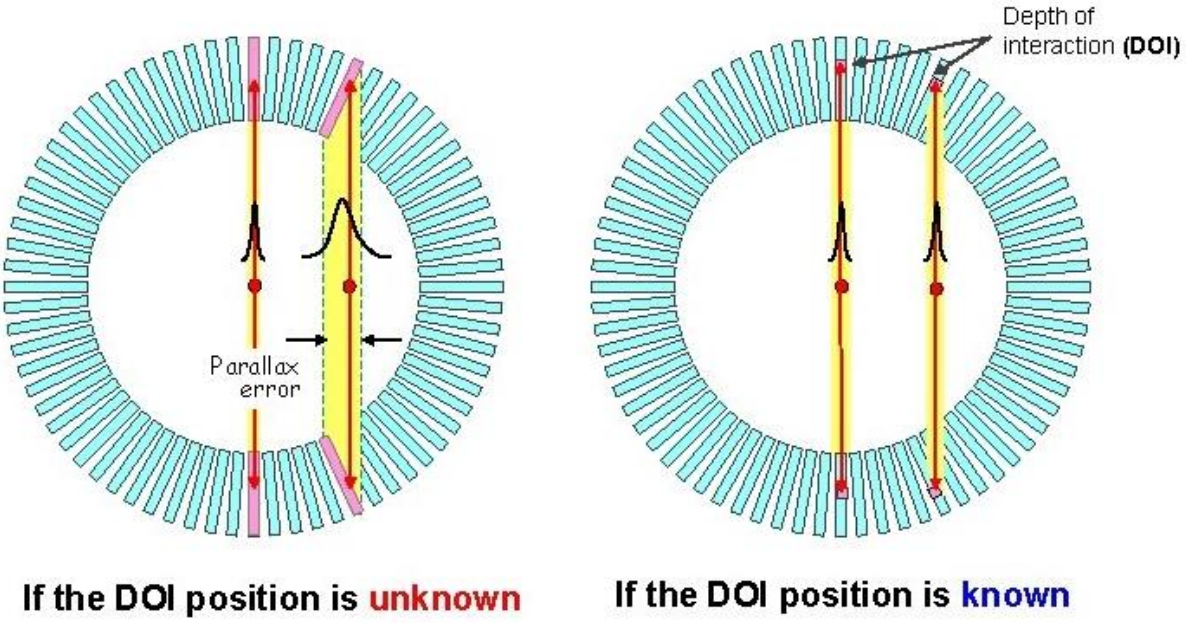

Figure 1.4 – Explanation of parallax effect

To reduce parallax effect scintillator thickness can be reduced, but the sensitivity in this situation reduced too. Also zero or close to zero thicknesses are ineffective and requires a lot of radioisotopes and time.

Second option of reducing parallax is DOI estimation. There are different approaches to solving of this problem such as [70]: multiple crystal layers (Figure 1.5 A); multiple layers of scintillator-SiPM couples (Figure 1.5 B); layers with different scintillators materials (Figure 1.5 C); dual-ended sensors readout (Figure 1.5 D), monolithic scintillator (Figure 1.5 E); phosphor-coating approach (Figure 1.5 F). Schematic presentation of approaches is presented in Figure 1.5 [39].

Multiple crystal layers with reflector can distinct different DOI layer based on knowledge what array pixels get light photons . Usually different layer offset relativity to each other in such way that the most deep layer can get counts only in one pixel, abortions in second layer lead to counting in 4 or more neighbor pixels and so on [71]. Number of DOI levels from 2 up 4 usually used.

With direct DOI encoding detector unit presented like stacked independent couples of readout electronic and scintillators [72, 73]. Such system obliviously can have high number of layers, but the number of sensors unit and corresponding channels of electronic increased highly and in consequence of this cost increased fast enough.

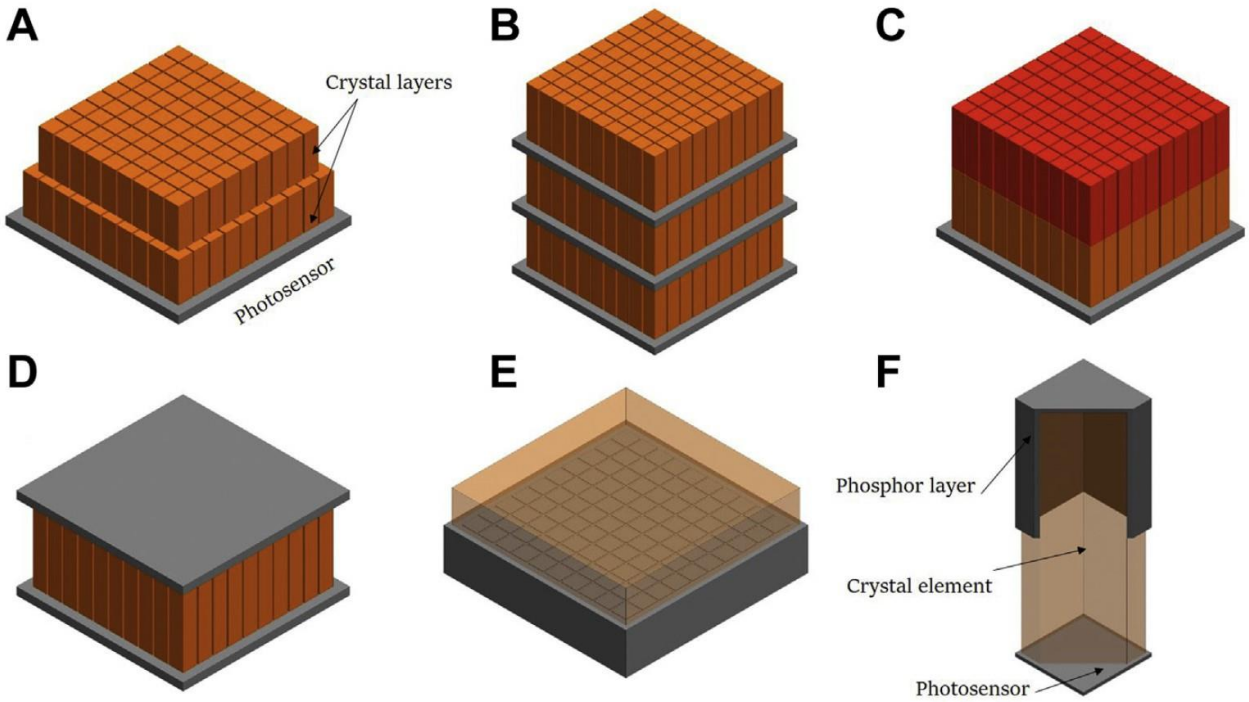

Figure 1.5 – Approaches for DOI encoding

Solutions with different scintillator materials layers usually named phoswich (phosphor sandwich) detectors. Phoswich detectors based on ability to distinct pulse time characteristics for different scintillators [74]. Often combination of materials are NaI(TI)/BGO and LSO/LuYAP [70].

Dual-readout approach based on evaluation of ration between two sides [75]. Some works show ability to get DOI resolution up to 2 mm [75]. It worth nothing that The cost of electronics doubled compare to single readout.

Monolithic scintillator [76] method has several important advantages for detection. Firstly, method is quite simple and cost-effective. The number of SiPMs are stay the same and scintillator has simple shape that is easier for production. Such configuration work based on collcted spectrum of light on SiPM. By the shape of distribution it is possible to make assumptions about DOI. Main problem of such method is distortion of resolution near to edges due to reflection. One of semi-solution is using absorption materials on surfaces.

In other approach phosphor coating modifies decay time of detected pulses such way that it depends on DOI [77]. With this method DOI resolution from 8 to 5 mm can be achieved.

2 PET Monte-Carlo simulation

2.1 General features of scanner

Based on observed variants, existing approaches and available channels number the next configuration was offered configuration that shown in Table 2.1.

Table 2.1 – Simulated PET general features

Feature	Solution
Scintillator material	LYSO
Electronic	d-SiPM
Performance accent	Spatial resolution
DOI evaluation	Monolithic scintillator
Plate channels	64
Number of all channels	1024

Monolithic scintillator approach was chosen due to easy manufacturing and not increasing of number of SiPMs. Also there are existing PET systems (Albira Si) with grate performance based on monolithic scintillator approach.

Based on features next detector's checkboard order and sparse plates were suggested. In Figure 2.1 is presented view of checkboard detector plate.

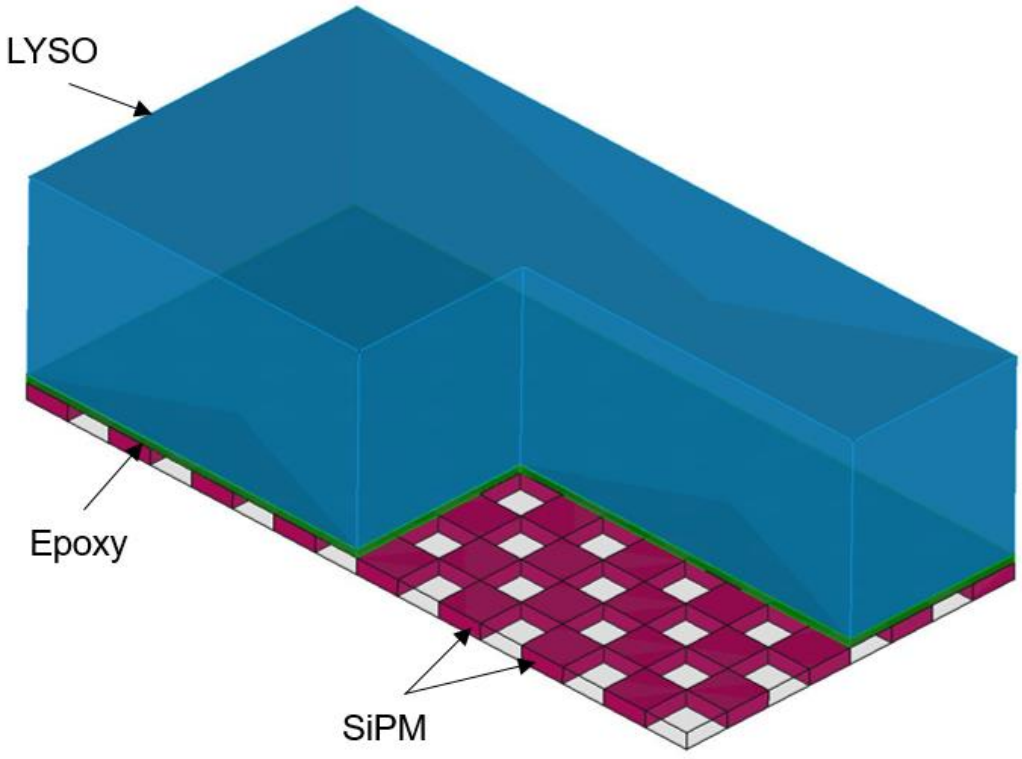

Figure 2.1 – Detector's plate with checkboard order, isometric view

The size of SiPM cells is 6 cm on 6 cm. Number of SiPMs are 16 along length and 8 along width. As with checkboard pattern the number of SiPMS will be the half from number of same dense array the result quantity of SiPMs is 16*8/2 = 64 that is perfect from condition of number of channels. Therefore, from number of SiPM is possible to get length and width of plate. Length is 16*6 = 96 mm and width is 8*6= 48 mm.

Due to empty spots in array, there are insensitive areas. Obliviously for detection of photons over empty space, the neighbor pixels should get some light. The lighted area is limited by internal reflection. In Figure 2.2 the geometry of reflection are presented.

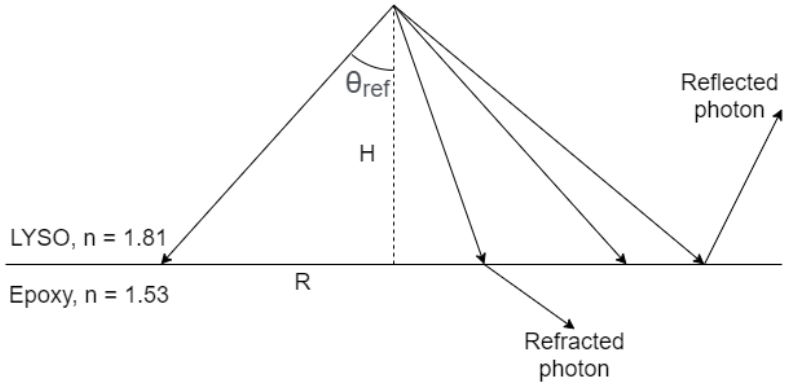

Figure 2.2 – Internal reflection on scintillator – epoxy border

Based on the geometry it is possible to get easy equation:

$$H = R \cdot ctg(\theta_{ref}) = R \cdot \frac{cos(\theta_{ref})}{sin(\theta_{ref})} = R \cdot \frac{\sqrt{1 - sin^2(\theta_{ref})}}{sin(\theta_{ref})}, \qquad (2.1)$$

where R – radius of area for corresponding height H, where inherent photon are not reflected;

θ_{ref} – total internal reflection angle for LYSO-Epoxy (scintillator- lightguide). With known refraction indexes the coefficient between radius and height is:

$$H = R \cdot \frac{\sqrt{1 - sin^2(\theta_{ref})}}{sin(\theta_{ref})}; \quad sin(\theta_{ref}) = \frac{n_{Epoxy}}{n_{LYSO}} => H = R \cdot \frac{\sqrt{n_{LYSO}^2 - n_{Epoxy}^2}}{n_{Epoxy}} = 0.632 \cdot R$$

where n_{Epoxy} – refractive index of epoxy (1.53);

n_{LYSO} – refractive index of LYSO (1.81).

According to formula angle of total internal refraction is 57.7 degrees and proportional index is 0.632.

Radius choosing of insensitive area depends on two criterions: direct sensitivity and uniformity of sensitivity. Based on first requirement the biggest insensitive area is when light photons emitted exactly above center of empty spot. As empty spot is square with side length 6 mm the radius of area is 3 mm. So height according to proportional index is 1.9 mm. It means around 2 mm height from LYSO/epoxy surface that is insensitive. However, with this height uniformity will not be same depending on XY position of interaction. Insensitive area should be close enough to included sensitive one without depending on XY position as much as possible. Uniformity in chosen area is ratio empty sum of empty spots and SiPMs. Of course because of limited sizes the radius should be lower than minimum sizes of array in our case it is width equal to 48 mm. Therefore, all calculation limited by minimum area and maximum area sizes.

Constituently, choosing of unused height is optimization problem, where parameters: sensitive area – maximized (sensitivity); fill factor (ratio of sensitive to all areas) – independent to XY shifting; radius – minimized. Last property chosen from point of cost efficiency and spatial resolution considerations. Due to discretization the problem of intersection circle with grid is has complex analytical solution [78]. The Monte-Carlo approach was used as solution for intersection area problem for simplicity of realization. Main change of fill factor value occurs when new sensitive square are included. So logically to suppose that positions of changing the monotone areas are on the node or spots where empty spots touches the empty spots, and opposite, where distance to nodes is maximum. Of course, such considerations do not guarantee the luck of extremum points and so on (Gauss circle problem [79]), but obliviously fill

factor limits to 0.5 and all difference to this point are decreasing with increasing of radius. However due to unnecessity of infinitive precision, the suggested algorithm covers all important variants. In Figure 2.3 the demonstration of calculated positions and dependencies of fill factor on radii are shown.

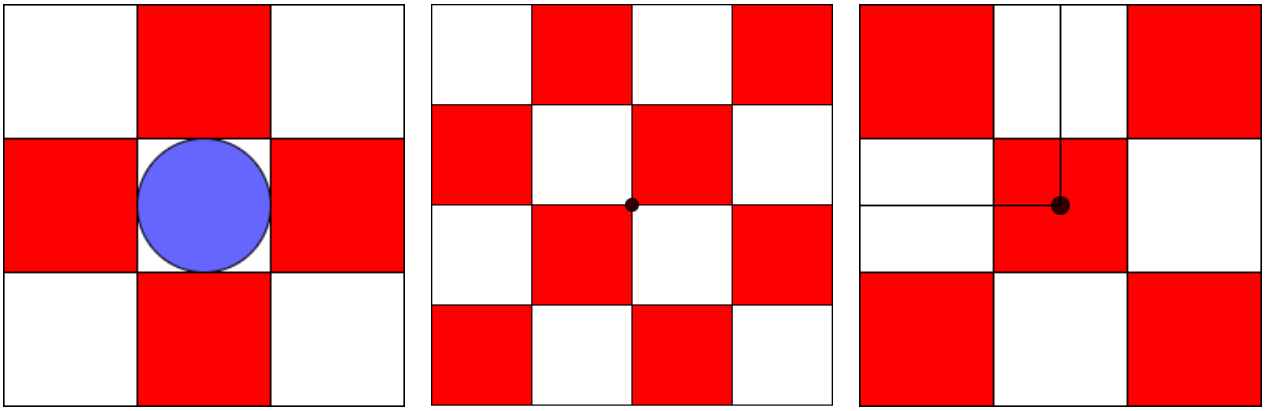

a) Illustration of minimal insensitive area (circle)

b) Observed point in center of cells intersection

c) Observed point in center of sensitive cell

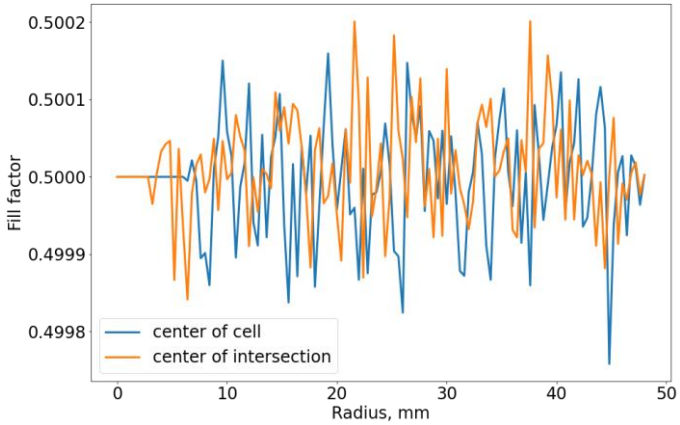

d) Fill factor depending on radius

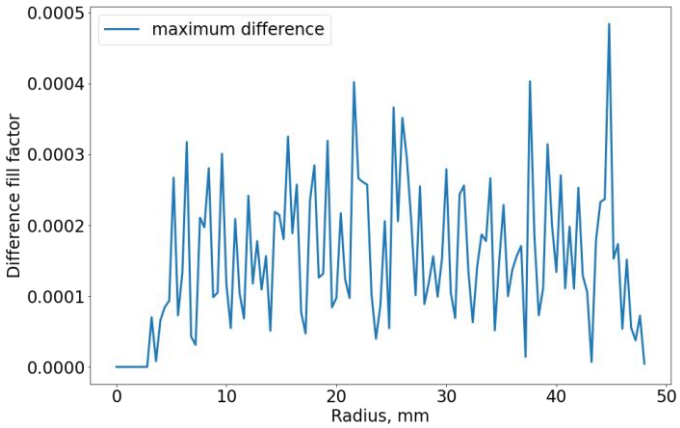

e) Maximum difference of fill factors for different point positions

Figure 2.3 – Uniformity calculation explanation and results

It is possible to see the results of Monte-Carlo calculation give very non-monotonic results. Firstly it could be related to relatively low statistics of measurements (10^7 per radius) or strong non linearity of Gauss circle problem. However, it worth nothing that for out task import order of difference. According to plot difference no exceeds the value with 0.0005, that is completely smaller relatively to ideal fill factor 0.5. Therefore, based on calculation it is possible to conclude, that influence of uniformity is negligible for considering.

After uniformity the only required factor is sensitivity, for minimal sensitive we are suggested a four minimal cells in grid 3x3 like in Figure 2.3 a). For such configuration minimum radius is about 8 mm. So, with coefficient 0.632 the height for required sensitive area is 5 mm.

After all evaluations, the useful thickness is about 5 mm. As LYSO has attenuation length 12 mm the thicknesses with 12 mm, 24 mm and 36 mm were chosen for comparison, but mainly 24 mm were observed more detailed because of most optimum thickness.

Second variant of plate configuration is sparse array of SiPMs. SiPMs sparse configuration is shown in Figure 2.4.

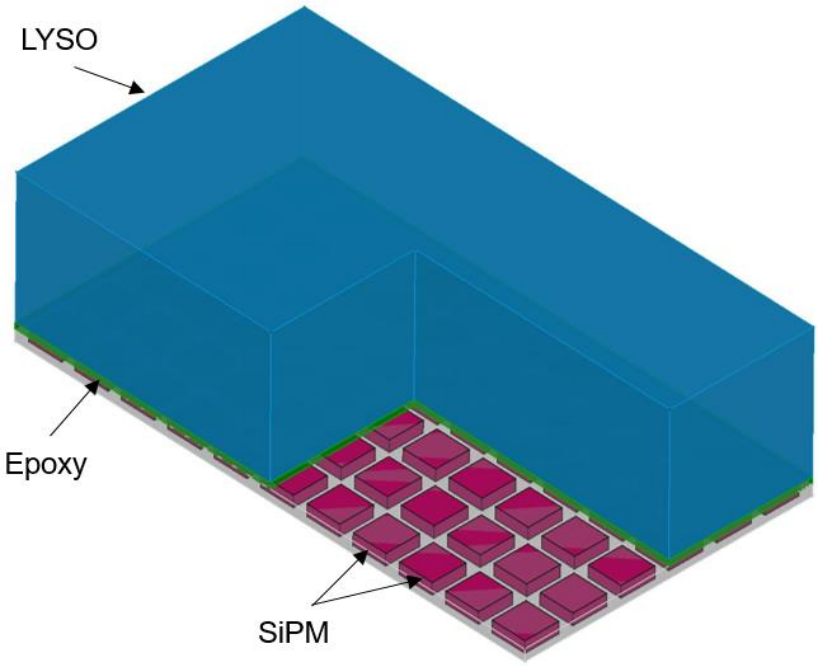

Figure 2.4 – Detector’s plate with sparse order, isometric view

Number of SiPMs are 11 along length and 6 along width. Such number were chosen for two reasons: ratio of axial FOV and transaxial FOV is close to 2 and the size of whole array close of checkboard option for better comparison. As sparse array has variable fill factor by changing the pitch (distance between pixells) the size of whole plate cold be varied. For first approach the array with fill factor 0.5 was chosen to correspond the checkboard variant. The pitch (P) can be found from cell size (c) and fill factor (φ) as:

$$P = \frac{c}{\sqrt{\varphi}} \tag{2.2}$$

As SiPM's pixels size is 6 mm, the evaluated pitch is 8.5 mm. With known pitch, the sizes of sparse plate are: 11x8.5=93.5 mm length and 6x8.5 = 51 mm. In general, the configuration was chosen in way of most adequate comparison of checkboard and sparse versions of configuration. The scintillator's thickness was chosen as 24 mm as for checkboard version.

The full detector is presented by 8 plates formed in rings, the number of rings variated, but most common variant with 2 rings. General detector geometry is shown in Figure 2.5.

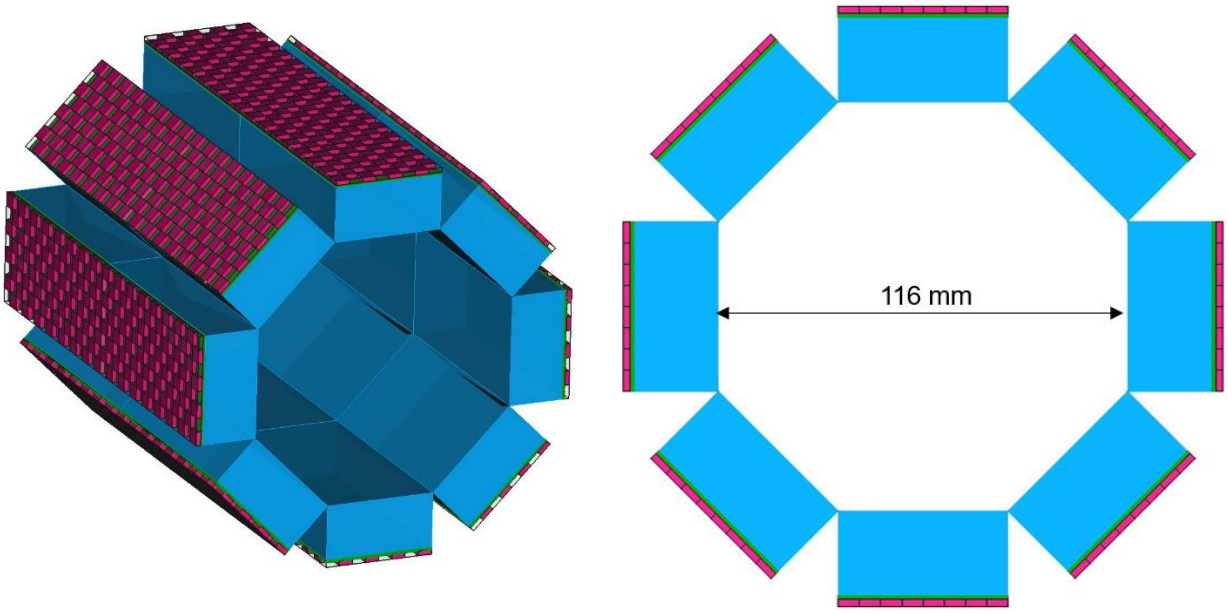

Detector isometric view Detector front view

Figure 2.5 – Full detector view

2.2 Detector’s physics simulation

For the simulation of PET system the Geant4 [80] was used. Geant4 is software toolkit for simulation of interaction of particles through matter. Geant4 is open-source, well-known and widely used software in physics simulation. In addition, one of the main advantages of Geant4 is comprehensive building of physics and flexible system of physics registration.

The most important processes for simulation of detector unit are electromagnetic and optical.

2.2.1 Electromagnetic processes

Geant4 has built physics packages. For base of physics the G4EmStandardPhysics_option4 [81] constructor.

For photon the next electromagnetic processes are included:

– Photo-electric effect

– Compton scattering

– Rayleigh scattering

Pair production of electron/positron is excluded due to energy of photons are not exceeds the rest energy of electron. For Compton scattering in G4EmStandardPhysics_option4 is used Monarsh University model [82]. For photo-electric effect and Rayleigh scattering the Livermore models are implemented [83].

For electron the next electromagnetic processes are included:

– Ionization and delta ray production

– Bremsstrahlung

– Multiple scattering

– Positron annihilation into two gammas

Multiple scattering is implemented through the Goudsmit-Sounderson model [84], which is c with the single Coulomb scattering model, which is applied for large angle

scatterings. UseSafetyPlus step limitation with error free approach near geometry boundaries is used for multiple scattering. The value of the Range Factor is 0.08. Bremsstrahlung is implemented by the eBremSB. Ionisation is modelled by the Moller-Bhabha formulation, and positron annihilation is implemented by the eplus2gg model.

Cross-sections for electromagnetic photon interaction processes as overage for LYSO and for it compartment elements are presented in Appendix B.

Other electromagnetic processes are not described here but included.

2.2.2 Optical processes

For simulation of optical photons next processes are included:

- Generation of optical photons
  - Scintillation
  - Cerenkov
- Optical photons interaction
  - Absorption
  - Rayleigh scattering
  - Boundary

Geant4 has not smooth transition between high energy photons and optical photons.

Also classical boundary optical interactions in Geant4 are included such as: reflection, refraction and absorption.

For light all the required properties should be defined such as: energy resolution, emission spectrum, light output, decay time, absorption length and refractive index of medium. In Appendix C the optical parameters for LYSO, epoxy and air are shown.

With 511 keV photons, the average number of created optical photons are: 0.511x33200 = 16965. High light yield means in one generated Geant4 event created around 17 thousands particles. This numbers shows that optical processes are quite expensive from point of calculation time. To reduce evaluation time can be used some

“trick”. Detection efficiency of SiPM is known from datasheet [85]. So way of reducing generated optical photons is taking detection efficiency of SiPM in generation. It is means to multiply corresponded wavelength LYSO emission value with SiPM efficiency. Such new updated spectrum will already include SiPM properties, but the scintillation light yield will reduce on SIPM efficiency coefficient. As SiPM J series has average value of efficiency about 50 %. The number of generated photons will reduced in half. However, with such approach need to carry about recalculating some properties and inability to use data for different SiPMs.

Fortunately, the surface of SiPM with index 1.53 and epoxy has the same index. So border of epoxy/SiPM could be observed as smooth transition of one medium. As there are approaches where wrappers or paints that change reflectivity and refraction properties [86, 87] the Geant4 provides logical surfaces which properties could be define manually with out material properties. But for the first iteration of work classical border were used by Snell’s low.

More detailed information about implemented physical models could be found in physics guide of Geant4 [88].

2.2.3 PET simulation physics verification

To verify the chosen physics of simulation, the simulation experiment was simulated. 551 keV photons bombards the thin layer of LYSO then all energy of all deposited particles is storage. The result of deposit spectrum is show in Figure 2.6.

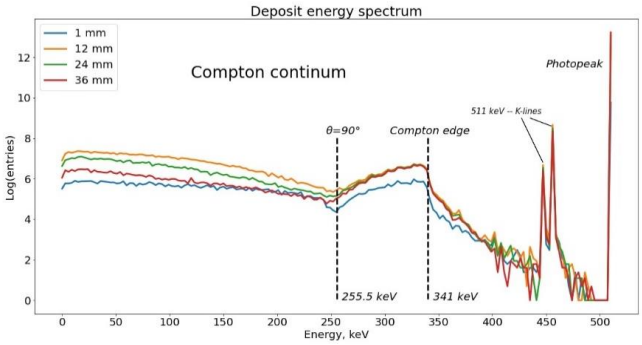

Figure 2.6 – LYSO energy spectrum deposition

Spectrum has all usual features of photon spectrum in scintillator. First of all

from 0 to 341 keV the Compton continuum is observed. Compton edge correspond to maximum energy with scattered angle is 180 degrees end can be calculated by equation:

$$E_{comp} = E_0 \cdot \left(1 - \frac{1}{1 + \frac{2 \cdot E_0}{m_e \cdot c^2}} \right) \quad (2.3)$$

where E_0 – the energy of photon before collision, in our case 511 keV;

$m_e c^2$ – rest energy of electron, 511 keV.

After calculation the evaluated Compton edge is 340.7 keV. In Figure 2.6 it is possible to see the edge correspond to theory. Also spectrum of Compton scattering corresponds to distribution by angle (the energy and angles are unambiguously interconnected) like Klein-Nishina distribution [89]. The fact, that the minimum of distribution in Compton range is in scattering angle = 90 degrees also correspond to classic spectrum.

Photopeak presented by line as in theoretically in ideal spectrum. In addition, there are smaller peaks. It is correspond the situation when photopeak occurs, but characteristics x-rays are fly out form scintillator with out absorption.

To sum up all of the above observing we can conclude that implemented physics proved by classical observed spectrum in scintillators.

The next step is absorption of electrons and optical photon creation. In Figure 2.7 the spectrum of summary energy of generated optical photons per one event is shown. As emission spectrum of LYSO is not ideal straight line (Appendix C.2) and has non-zero energy resolution the photopeak is presented by like similar to Gauss shape. Usually part of spectrum related to photopeak is considered as full width at half maximum (FWHM). Based on spectrum data it is possible to define energy window equal FWHM. As shown the ratio of photopeak to Compton increasing with increasing of thickness of scintillator. But for all thicknesses excepting 1 mm the ratio is high enough.

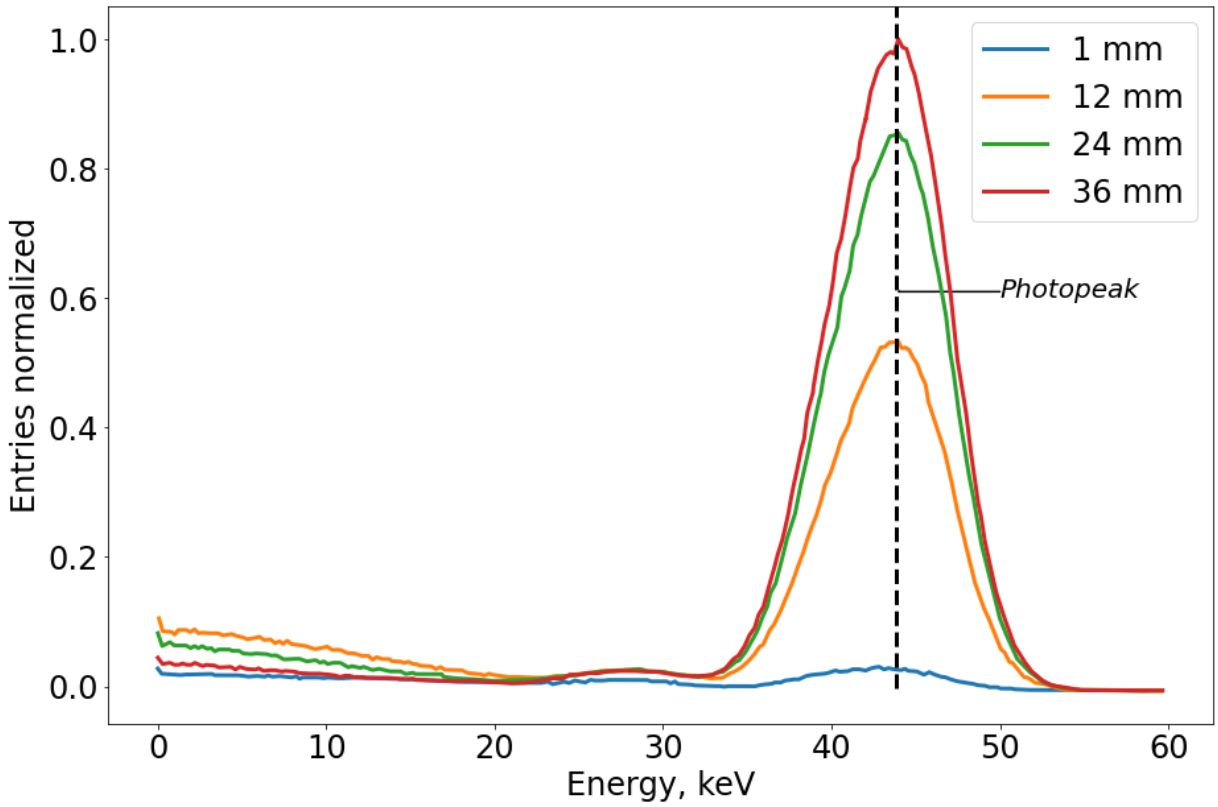

Figure 2.7 – Summary energy distribution of generated optical photons

So, main interaction processes are based on electromagnetic and optical processes.

2.3 PET scintillation events simulation

To estimate some performance properties is necessary to collect some statistics and also observing of characteristic images. In Appendix D the main results of events simulation are shown for dense matrix.

In Appendix D.1 the average distribution on SiPMs is shown. It is possible to see that distribution is has Gauss shape like. According to theory, the distribution should have the Cauchy distribution [90]. Appendix D.1 shows, that with increasing of DOI the maximum value increased and distribution has more narrow shape. As spectrum it is overage value the noises and another distortion factors are excluded effectively. The peak registered number is about 250 counts.

In Appendix D.2 results of absorption near to the surface are shown. It is possible to see that now distribution not so smooth but the maximum point is still

recognizable. The name corner 1 is correspond to checkboard order as in chess, and for corner 2 the empty spots and SiPMs are replaced by each other. The XY position of is determined by weighted average. As the distance between scatterings is small in Appendix D.2. the results are the same for dense SiPM's array and checkboard version both versions. It means results are well when scattering in small.

In Appendix D.3 same simulation demonstrated as for Appendix D.2, but with thickness of LYSO scintillator 36 mm. As seen in Appendix D.3 and Appendix D.2 the summary counts are increased well with increasing of thickness that is expected. But results of calculations shows that with 36 mm of thickness calculation gives the results with errors of same orders as for 24 mm. This means of course that if distance between scattering is small enough the results will be good for high range of scintillator thicknesses.

In Appendix D.4 results of absorption are deep enough. In addition, distance between initial interaction and absorption is long. As seen on figure the distribution on SiPM's array looks like no circle shape like, but stretched. As all interactions is near the LYSO/SiPMs surface, the distribution take small area, narrow shape and maximum value is high. Comparison of results shows the difference of calculation from ground truth more then 1 mm and 3 mm. It is means when distance to between interactions high enough, the only weighted mean algorithm shows relatively rough results. For such purposes is necessary to cluster distribution of the sources like classical k-NN method [91]. But interesting moment that checkboard version of array shows same orders of results and it is possible to conclude that empty sport not add any distortion to results even if interaction close to array.

In Appendix D.5 same simulation demonstrated as for Appendix D.4, but with thickness of LYSO scintillator 36 mm. As seen in Appendix D.4 the distribution now more stretched and Gauss shape observed more well. In addition, the distribution has more noise behavior. But results of calculations shows that with 36 mm of thickness calculation gives the results with errors of same orders as for 24 mm. This means that if distance between scattering is high enough the results will be not so close for high range of scintillator's thickness and this not depends on checkboard or spare

arrangement of SiPMs array.

2.3.1 Estimation of scattering effect in position evaluation

As determination of one point of absorption is not complex and well precision task, the main problem is scattering, as shown in previous paragraph in satiation when distance between scattering point is high, the determination of XY position is hard. However, before the determination error estimation, necessary to define how far absorption point could be to each other. This parameter mainly depends on physic properties of system. In Figure 2.8 the cumulative distribution of maximum distance between interaction is shown.

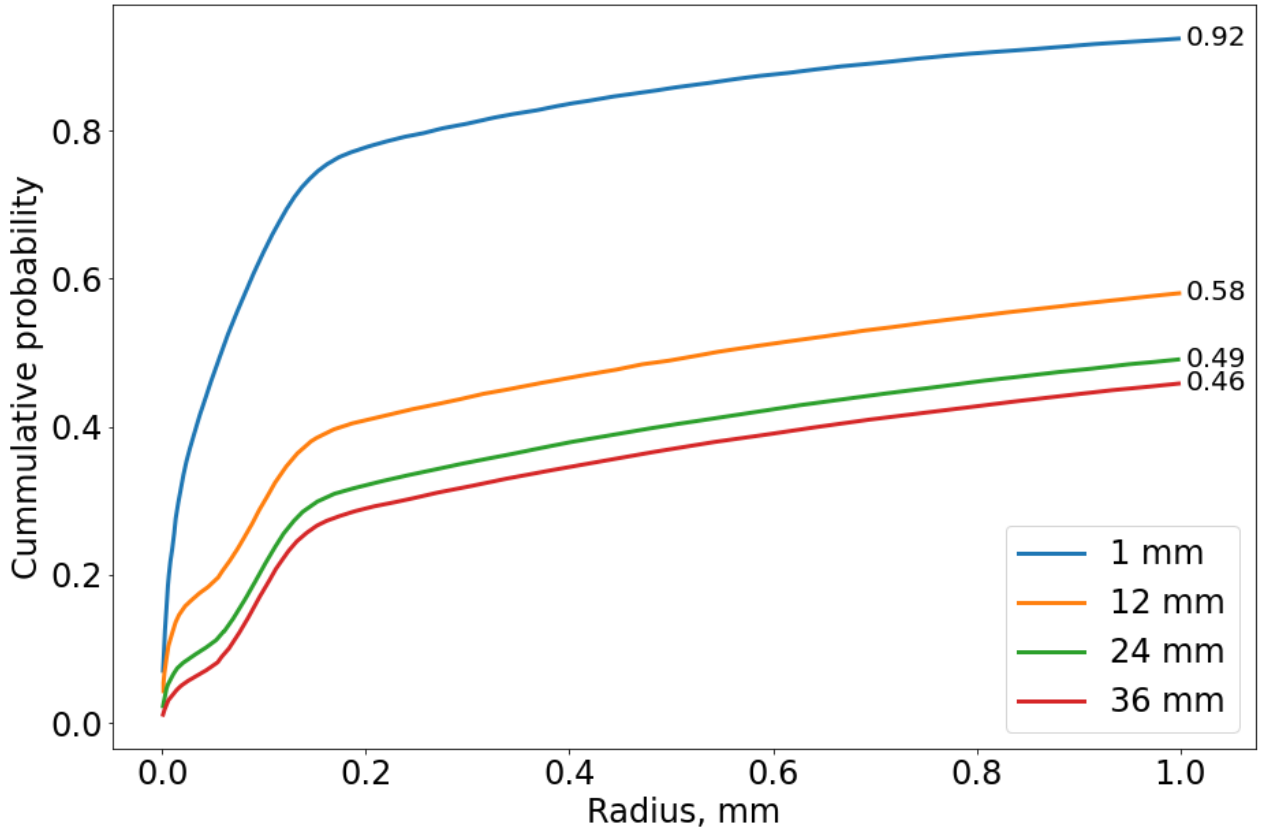

Figure 2.8 – Cumulative probability of maximum distance between interactions

On the Figure it is seen that for 24 mm half of all events will be with scattering no more than 1 mm. So if our goal to achieve resolution about 1 mm, the half of events will be useful and others needs to be excluded or processed with more modern

approaches. It is possible to see that with increasing of thickness of material, the probability of maximum distance under 1 mm is decreased. The expected value of all distribution is around 0.11 – 0.13 mm. Consequently, the scattering allows to determine the XY position under 1 mm.

The behavior of the curve is high increasing before 0.1 mm and slow increasing after 1 mm. As seen on the Figure for 12 – 36 mm thickness under 0.1 mm the slope changes and for 1 mm thickness slope the monotonically the same. It can be explained with fact that the sizes of scintillator plate is finite by width and length. And after scattering photon fly out of the LYSO without interaction.

2.3.2 Photon interaction position estimation

In this work results of XY position calculation were analyzed. In Figure 2.9 The distribution of calculated X position is shown. The ground truth position is in center of checkboard array (true X = 0).

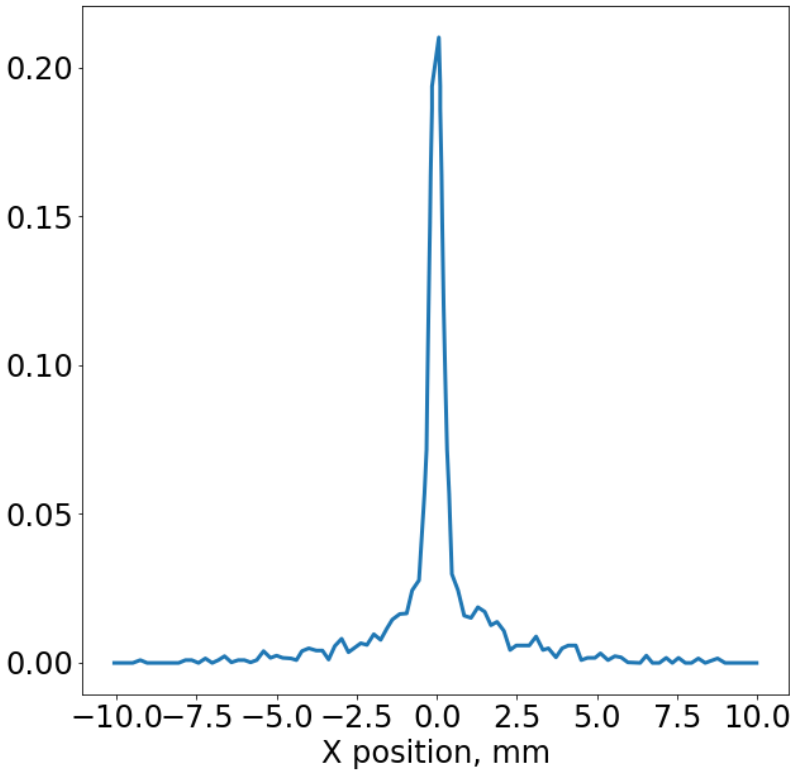

Figure 2.9 – Estimated X position distribution for checkboard array

The standard deviation of distribution is around 0.8 mm. The results shows that distribution has narrow shape and most of calculated results under 1 mm.

In addition, the cumulative function of distribution is shown on Figure 2.10.

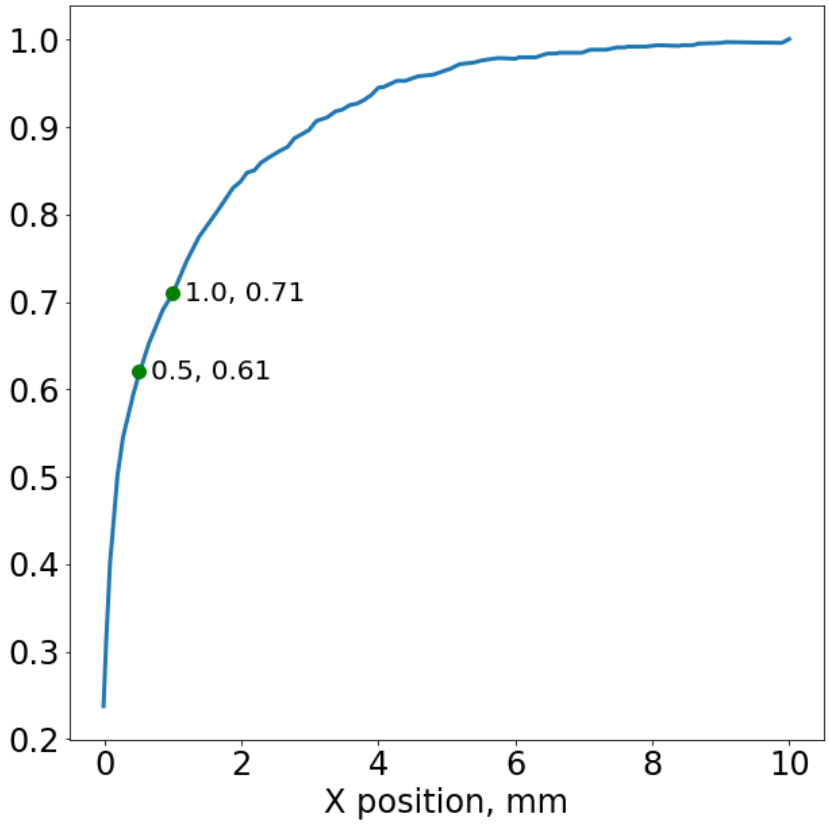

Figure 2.9 – Estimated X position cumulative distribution for checkboard array

As seen on Figure 2.9 the 71 % of all events were determined with difference less than 1 mm from center. In addition, the 61 % were estimated with difference less than 0.5 mm. Therefore, even most primitive calculation way gives good results.

It is also interesting how probability distributed by DOI. On Figure 2.10 the probability that detected photon will be determined under 1 mm for different thicknesses is shown. It is possible to see that the probability of determination is increased in the beginning of DOI and in the end. In the middle region of scintillator height the probability decreased. It can be explained by geometry considerations. As DOI is higher, the point of interaction is getting closer and determination of position is more precise. Increasing at the beginning occurs due to excluding of photon scattered back from initial direction. Back scattered photon just fly out of volume without

absorption and scattering length is decreased. As seen for all thicknesses the probability of estimation of photon under 1 mm is higher than 70 %.

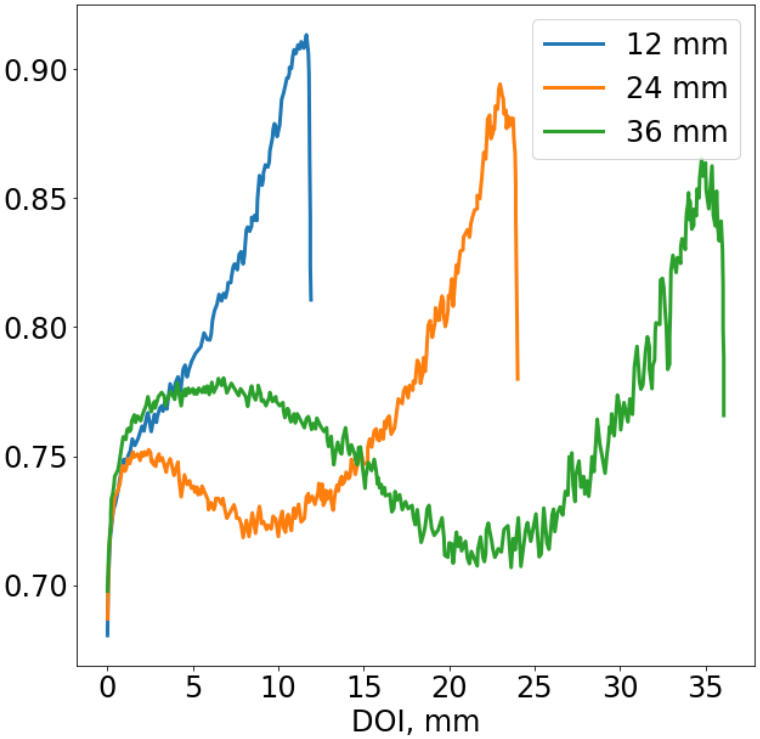

Figure 2.10 – Estimated X position cumulative distribution for checkboard array

To observe not only probability but physical properties the root mean square error (RMSE) depending on the DOI for different thicknesses. The results are shown on Figure 2.11 (CB is checkboard).

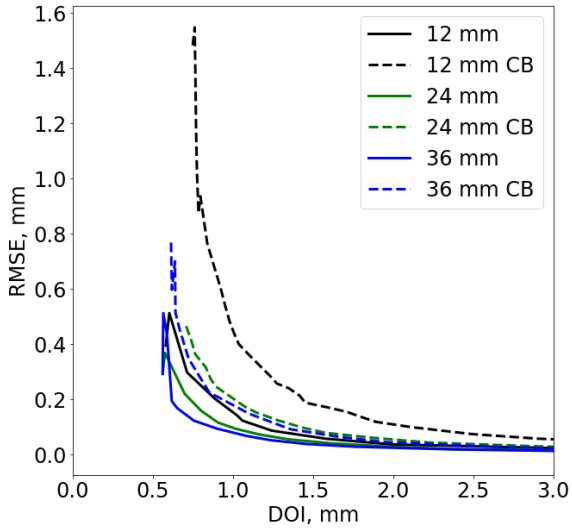

Figure 2.11 – Root mean square error depending on DOI

The results of calculations demonstrate decreasing of XY RMSE with increasing of DOI. In addition, on Figure 2.11 is seen that checkboard version increase the RMSE of estimation. Also bigger thickness gives less RMSE of results.

3 Financial management, resource efficiency and resource saving

3.1 Project initiation

Initiation processes define initial goals and content and fix initial financial resources. The internal and external stakeholders of the project are determined, which will interact and influence the overall result of the scientific project.

3.1.1 Project goals and results

Table 3.1 – Stakeholders of the project

Stakeholders of the project	Stakeholders of the project expectations
Medical scientific centers, medical equipment manufactures.	Low cost of experiment; Flexible experiment modification system; High precision of results

Information about the stakeholders of the project, the hierarchy of project goals and criteria for achieving goals is presented in upper table.

Information about the hierarchy of project goals and criteria for achieving goals is given in the table below.

Table 3.2 – Project goals and results

Project goals	Digital twin model of small-animal PET system for effective performance predictions and optimization of system characteristics.
Expected results of the project	Monte-Carlo simulation with flexible experimental settings and well consistency with real world.
Acceptance criteria of the project result	High precision of experiments and enough statistics
Requirements to the project results	Project completion on time
	Stability of simulation provided
	The efficiency of the simulation

3.1.2 Organization structure of the project

Table 3.3 – Project Working Group

№	Name	Position	Functions	Hours spent
1	Alekseev N.V.	Student	Work on project implementation	800
2	Gogolev A.S.	Superviser	Coordination of work activities and assistance in project implementation	140
3	Engineer	Engineer	Building of PC equipment	7
Total:				1147

The organizational structure of the project is presented in the Table 3.3.

Engineer Filatov Nikolay Aleksandrovich is employer from research unit of TPU “X-Ray Optics International Lab”. As all equipment for work belongs to laboratory, the building of PC was done by laboratory specialist.

3.1.3 Assumptions and constraints

Table 3.4 – Limitations and assumptions

Factor	**Limitations/assumptions**
1. Project budget - for PC and design	593401 RUB
1.1 Source of budgeting	Customers
2. Project timeline:	1 Febuary 2021 – 30 May 2021
2.1 Date of approval of the project management plan	05 February 2020
2.2 Project completion date	30 May 2020
3. Other	-

Limitations and assumptions are summarized in upper table.

As a result of the initialization of the project, the goals and expected results were formulated, the stakeholders of the project and the financial framework were identified, which is important for the completion of the project and its implementation.

3.1.4 Project planning

Deadlines for the project stages are listed in Table 3.5. In addition, Table 3.6 visualized project schedule in form of bar chart also called Gantt chart

Table 3.5 – Project timeline

Job title	Duration, working days	Start date	Date of completion	Participants
Building PC	1	01.02.2021	02.02.2021	Engineer
Drawing up the technical assignment	4	01.02.2021	05.02.2021	Supervisor
Calendar planning	4	06.02.2021	10.02.2021	Supervisor, Student
Literature review	13	11.02.2021	24.02.2021	Student
Choosing of PET configuration	3	25.02.2021	28.02.2021	Supervisor, Student
Detector unit Geant4 implementation	20	01.03.2021	21.03.2021	Student
Evaluation of detector unit performance	10	21.03.2021	31.03.2021	Student
Updating of PET configuration	10	01.04.2021	11.04.2021	Supervisor, Student
Phantoms Geant4 implementation	11	12.04.2021	23.04.2021	Student
PET system Geant4 implementation	15	24.04.2021	09.05.2021	Student
Evaluation of PET system performance	10	10.05.2021	20.05.2021	Student
Summarizing	2	21.05.2021	23.05.2021	Supervisor, Student
Drawing up a final report	6	24.05.2021	30.05.2021	Student

Table 3.6 – Schedule of the project design

№	Activities	Participants	T_c, days	Duration of the project															
				February				March				April				May			
				1	2	3	4	1	2	3	4	1	2	3	4	1	2	3	4
1	Building PC	Engineer	1																
2	Drawing up the technical assignment	Supervisor	4																
3	Calendar planning	Supervisor, Student	4																
4	Literature review	Student	13																
5	Choosing of PET configuration	Supervisor, Student	3																
6	Detector unit Geant4 implementation	Student	20																
7	Evaluation of detector unit performance	Student	10																
8	Updating of PET configuration	Supervisor, Student	10																
9	Phantoms Geant4 implementation	Student	11																
10	PET system Geant4 implementation	Student	15																
11	Evaluation of PET system performance	Student	10																
12	Summarizing	Supervisor, Student	2																
13	Drawing up a final report	Student	6																
* T_c – calendar days																			
Supervisor		Student		Engineer															
Total duration: Alekseev N.V. (Student) – 104 days, Gogolev A.S. (Supervisor) – 23 days, Engineer – 1 day																			

3.1.5 Project budgeting

The project budget must display reliable values for all types of costs associated with its implementation. The costs of this project include:

– Costs of purchasing equipment;

– Costs of additional materials;

– Expenses for the main and additional salaries of the theme performers;

– Costs of social security contributions;

3.1.5.1 Costs of purchasing equipment

Due to digital twin concept only PC equipment required.

Table 3.7 shows needful basic equipment and accessories, and also its cost for scientific work.

Table 3.7 – Cost of equipment and accessories for project

Name of equipment	Quantity, units	Price per unit, tsd rub	Total cost for position, tsd rub
CPU	1	95	95
Motherboard	1	30	30
CPU Cooler	1	11	11
Memory module	1	66	66
Power supply	1	15	15
SSD	1	12	12
Computer case	1	4	4
GPU	1	7	7
Monitor	1	25	25
UPS	1	6	6
Electricity			3
Total:			274

All transportation costs already are included in price of equipment.

Electricity cost are calculated by formula:

$$C = P_{el} \cdot P \cdot F_{eq}, \quad (3.1)$$

where P_{el} – power rates (5.8 rubles per 1 kWh);

P – power of equipment (0.65 kW);

F_{eq} – equipment usage time, hours. (800 hours);

So, cost of power for project time is about 3016 rubles.

Depreciation is the gradual transfer of costs incurred to purchase or build property, plant and equipment to the cost of the finished product. With its help, money spent on the construction or purchase of property is compensated. Depreciation deductions are paid during the entire period of property exploitation.

Working time deprecation for PC as an whole was calculated with linear equation:

$$\frac{C \cdot T_w}{T_{full} \cdot 365} \quad (3.2)$$

where C – Price of PC (271000 rubles);

T_w – working days (104 days);

T_{full} – life time of equipment (7 years).

Final deprecation for working period according to (3.2) is 11031 rubles.

All required software and operation system are open-source, which cost for this no needs to include.

3.1.5.2 Costs of additional materials

Table 3.8 shows needful other materials for scientific work. These costs include office supplies, printing costs and various equipment required for research except specialized equipment.

Table 3.8 – Cost of additional materials for project

Name	Unit of measurement	Number	Price per unit, RUB	Expenses (E_M), RUB
Paper	Pack	1	250	250

Name	Unit of measurement	Number	Price per unit, RUB	Expenses (E_M), RUB
Pens	Unit	2	50	100
Pencils	Unit	1	50	50
Ruler	Unit	1	40	40
Printing	Page	100	2	200
Folder	Unit	2	5	10
Total				425

3.1.5.3 Salary

The amount of expenses for wages of employees is determined based on the labor intensity of the work performed and the current system of salaries and tariff rates.

The calculation of the basic salary of the head of a scientific project is based on the sectoral wage system. The branch system of remuneration at TPU assumes the following composition of wages:

- Salary - determined by the enterprise. In TPU, salaries are distributed in accordance with the positions held, for example, assistant, art. lecturer, associate professor, professor (see "Regulations on remuneration" given on the website of the Planning and Finance Department of TPU).
- Incentive payments - set by the head of departments for effective work, performance of additional duties, etc.
- Other payments; district coefficient.

Since incentive bonuses, other payments and incentives depend on the activities of the manager in particular, we will take the coefficient of incentive bonuses (k_b) equal to 30%, and the coefficient of incentives for the manager for conscientious work (k_{pr}) activity is 25%, regional coefficient (k_r) – 1.3.

Average daily salary S_d for a 5-day working week:

$$S^d = \frac{S}{F_d} \tag{3.3}$$

where S – monthly salary, rub;

F_y – average number of working days in a month;

Monthly salary with bonuses S_M can be calculated using formula:

$$S_M = S_b \cdot (1 + k_{pr} + k_b) \cdot k_r \quad (3.4)$$

where S_b – basic monthly salary, rub.

Additional monthly salary:

$$S_{add} = k_{extra} \cdot S_M \quad (3.5)$$

where k_{extra} – additional salary coefficient (10-15%). For calculation values 10% is used.

Average number of working days in a month F_d was determined as:

$$F_d = \frac{D}{M} = \frac{247}{12} \approx 20.58 \quad (3.6)$$

where D – number of working days in year (247 days);

M – number of months in year (12);

Salary for working period T can be determined through daily salary S^d as:

$$S^W = S^d \cdot T \quad (3.7)$$

The full salary for working period is:

$$S^W_{full} = S^W_M + S^W_{add} \quad (3.8)$$

where $S_M{}^W$ – salary with bonuses for working period, rub;

$S_{add}{}^W$ – additional salary for working period, rub.

Table 3.9 shows calculated salary values for Supervisor and student. Student was equalized to engineer-researcher. S^d_M and S^d_{add} are daily corresponding salaries. Engineer in this project has one-time job. Salary for building PC by engineer costed 1000 rubles.

Table 3.9 – Salaries of participants in the project

Participants	S_b, rub	S_M, rub	S_{add}, rub	S^d_M, rub	S^d_{add}, rub	T, days	S^W_M, rub	S^W_{add}, rub	S^W_{full}, rub
Gogolev A.S.	45000	90675	9068	4406	441	18	79308	7931	87239
Alekseev N.V.	20000	40300	4030	1958	196	69	135117	13512	148629
Engineer									1000
Total:									236868

3.1.5.4 Contributions to social funds

Here I will consider the obligatory contributions according to the norms established by the legislation of the Russian Federation to the state social insurance bodies (FSS), the pension fund (PF) and medical insurance (FFOMS) from the costs of wages of employees. The amount of contributions to extra-budgetary funds is determined by the formula:

$$S_{soc} = k_{soc} \cdot S_{full}^{W} \tag{3.9}$$

where k_{soc} – contribution rate to extrabudgetary funds.

In accordance with Federal Law № 212-FL of 24.07.2009, the amount of insurance premiums is set at 30 %. Table 3.10 shows contributions to social funds.

Table 3.10 – Contributions to social funds

Participants	*S*, rub	k_{exb}	S_{exb}, rub
Gogolev A.S.	87239	30%	26172
Alekseev N.V.	148629		44589
Engineer	1000		300
Total:			71061

3.1.5.5 Formation of the budget of the costs of a research project

Table 3.11 – The total budget of research

Name	Cost, rub	Cost, %
Costs of purchasing equipment	274016	46.17
Deprecation of equipment	11031	1.86
Costs of additional materials	425	0.07
Supervisor salary costs	87239	14.70
Student (Researcher) salary costs	148629	25.05
Engineer	1000	0.17
Contributions to social funds	71061	11.98
Research budget	593401	100

3.2 Economic model development

3.2.1 Competitiveness analysis of technical solutions

Analysis of competitive technical solutions in terms of resource efficiency and resource saving allows to evaluate the comparative effectiveness of scientific development. This analysis is advisable to carry out using an evaluation card.

Technical performance of project strongly depends on CPU power. For this work Three configurations were selected: CPU Ryzen 9 5950X, CPU Ryzen 7 5800X and real detector.

The position of the development and competitors is assessed for each indicator by an expert method on a five-point scale: 1 – the weakest position, 5 – the strongest. The weights of the indicators, determined by expert judgment, should add up to one.

The analysis of competitive technical solutions is determined by the equation:

$$C = \sum_i P_i \cdot W_i \tag{3.10}$$

where C – the competitiveness of research or a competitor;

W_i– criterion weight;

P_i – point of i-th criteria.

The Table 3.12 shows comparison of three solutions: index f means Ryzen 9 5950X, $i1$ – Ryzen 7 5800X, $i2$ – real detector.

By comparison, Ryzen 9 5950X shows the best results but Ryzen 7 5800X has close results and same orders of values. Real detector has much lower results due to concept of project and importance of mutability of configuration in development step.

Table 3.12 – Evaluation card for comparison of competitive technical solutions

Evaluation criteria	Criterion weight	Points			Competitiveness		
		P_f	P_{i1}	P_{i2}	C_f	C_{i1}	C_{i2}
1	2	3	4	5	6	7	8
Technical criteria for evaluating resource efficiency							
1. Mutability of configuration	0.4	5	4	1	2.00	1.60	0.4
2. Development time	0.05	5	5	1	0.25	0.25	0.05

1	2	3	4	5	6	7	8
3. Experiment time	0.05	3	2	5	0.15	0.10	0.25
4. Consistency	0.1	3	3	5	0.30	0.30	0.50
5. Preparation time	0.05	5	5	3	0.25	0.25	0.15
6. Safety	0.01	5	5	4	0.05	0.05	0.04
Economic criteria for performance evaluation							
1.Development cost	0.1	5	5	1	0.50	0.50	0.10
2.Price	0.2	4	5	1	0.80	1.00	0.02
3. Usability for other projects	0.04	5	5	5	0.20	0.20	0.2
Total	1	40	39	26	4.50	4.25	1.71

3.2.2 SWOT analysis

Complex analysis solution with the greatest competitiveness is carried out with the method of the SWOT analysis: Strengths, Weaknesses, Opportunities and Threats.

Table 3.13 presents the final SWOT-analysis matrix.

Analysis of SWOT matrix shows that combantion of working on opportunities with weaknesses has more reliable options. Also strength features of project works with opportunities and threats as well. The lowest number of variants with combination of weaknesses and threats.

Table 3.13 – SWOT-analysis

	Strengths: S1. Possibility to change configuration. S2. Low cost of one experiment. S3. Low cost of equipment. S4. Portability on other devices. S5. Low preparation time.	Weaknesses: W1. Experiment requires a lot of time. W2. Consistency lower than real. W3. After project the real detector required anyway.
Opportunities: O1. Accelerating calculation of experiment. O2. Improving of consistency. O3. Improving of equipment.	S1O1. Providing of high flexible and fast simulation to reduce number of possible variants of configurations. S4O1. Reducing of transport cost through internet transition of model. S4O3. Using cloud calculation	W1O1. Using of calculation tricks to speed up experiment time. W2O2. Using some empirical knowledge to improve consistency. W3O3. PC devices can be chosen for next usage as part of

	power as equipment.	detector. W1O3. Improving of CPU can significantly reduce calculation time.
Threats: T1. Calculation time to long. T2. Model will be not enough accurate. T3. Disability to include some real property.	S1T2. Exclude insignificant properties after testing different close configurations. S1T3. Tune configuration using known empirical data. S5T1. Using some tricks before each experiment.	W1T1. Necessary of reducing time performance. W3T3. Combination of simulation knowledge and real detector results.

3.2.3 Methods of commercialization of the results of scientific and technical research

Due to high price of final PET system (over 150 million rubles), any event of selling vary unique and highly depends on customer and developer. But for most common situation know-how is preferred as most flexible type for this purpose.

3.3 Evaluation of the comparative efficiency of the scientific research project

Determination of efficiency is based on the calculation of the integral indicator of the effectiveness of scientific research. Its finding is associated with the determination of two weighted averages: financial efficiency and resource efficiency.

Integral financial indicator I_f^p of a scientific research is obtained in the course of assessing the budget of the costs of three (or more) variants of the implementation of a scientific research. For this, the largest integral indicator of the implementation of a technical problem is taken as the calculation base (as the denominator), with which the financial values for all execution options are correlated.

Integral financial indicator I_f^p of current project is determined in the equation:

$$I_f^p = \frac{F_{pi}}{F_{\max}} \ , \tag{3.11}$$

where F_{pi} – price for *i*-th variant of execution;

F_{max} – maximum cost of execution of a research project (including analogs).

The resulting value of the integral financial indicator of development reflects the corresponding numerical increase in the budget of development costs in times (a value greater than one), or the corresponding numerical reduction in the cost of development in times (a value less than one, but higher than zero).

The integral indicator of the resource efficiency I_m^p, I_m^a of the variants of the object of research can be defined as follows:

$$I_m^a = \sum_{i=1}^{n} a_i \cdot b_i^a \ , \tag{3.12}$$

$$I_m^p = \sum_{i=1}^{n} a_i \cdot b_i^p \ , \tag{3.13}$$

where a_i – the weight coefficient of the ith parameter;

b_i^a, b_i^p – the score of the ith parameter for the analog and development, set by an expert method on the selected rating scale, index *a* means alternative, *p* – project;

n – the number of comparison parameters.

For comparative analysis were chosen CPU Ryzen 9 5950X, CPU Ryzen 7 5800X and real detector as in chapter 3.2.1.

Table 3.14 – Comparative evaluation of the characteristics of the project

Criteria	Weighting factor	Scientific research project (Ryzen 9 5950X)	Alternative 1 (Ryzen 7 5800X)	Alternative 2 (Real detector)
1. Mutability	0.3	5	5	1
2. Execution time	0.2	3	2	5
3.After usability	0.2	5	4	5
4. Workers qualification	0.1	4	4	2
5. Consistency	0.2	3	3	5
Total:	1	20	18	18

An integral efficiency indicator of the scientific research project I_{fin}^{p} and of the analog I_{fin}^{a} are determined according to the formula of the integral basis of the financial integral resource efficiency:

$$I_{fin}^{a} = \frac{I_{m}^{a}}{I_{f}^{a}} \tag{3.14}$$

$$I_{fin}^{p} = \frac{I_{m}^{p}}{I_{f}^{p}} \tag{3.15}$$

Comparison of the integral indicator of the efficiency of the current project and analogs will determine the comparative efficiency the project. Comparative project efficiency E_{av} :

$$E_{av} = \frac{I_{fin}^{p}}{I_{fin}^{a}} \tag{3.16}$$

All calculated indicators are listed in Table 3.15.

Table 3.15 – Comparative project efficiency

№	Indicator	Project,	Alternative 1	Alternative 2
	Final cost, rub	593401	545401	58632548
1	Integral financial indicator I_{f}^{p}	0.01	0.009	1
2	Integral resource efficiency indicator I_{m}^{p}, I_{m}^{a}	4.1	3.7	3.5
3	Integral efficiency indicator I_{fin}^{a}, I_{fin}^{p}	408.4	401.2	3.5
4	Comparative evaluation of the project execution variants	Alternative 1: 1.02 Alternative 2: 116.69	Alternative 2: 114.63	Alternative 1: 0.01

Comparison of the integral indicator allows to understand and choose a cheaper option for solving the technical problem in terms of financial and resource efficiency. As a result, we can conclude that the most optimal option is CPU Ryzen 9 5950X.

3.4 Conclusion

In this financial section, the general organizational and planning stage were determined. For effective time managing of project, the Gantt diagram was constructed.

In addition, the cost required for project were calculated. Summary cost was divided onto such groups as: purchasing equipment, additional materials, salaries, social security contributions. After all calculations, the final budget of project was evaluated as 593401 rubles.

Finally, economic potential of project was observed. Competitive analysis was provided and results show PC with CPU Ryzen 9 5950X as best option for project. For developing of project SWOT matrix was constructed. The most varies way according to SWOT is use opportunities of improvement to reduce weaknesses of project. As final parameter the comparative efficiency was evaluated and shown well results.

4 Social responsibility

4.1 Introduction

Price of small-animal PET system is high enough (over 150 million rubles). That is why important to know performance and optimize configuration of PET system to exclude overhead on building step. Digital twin one of the solutions of this problem. Simulation of PET system on PC cost much lower than real detectors and allows changing configuration fast. In this work Monte-Carlo PET simulation is provided.

4.2 Legal and organizational items in providing safety

Nowadays one of the main ways to radical improvement of all prophylactic work referred to reduce Total Incidents Rate and occupational morbidity is the widespread implementation of an integrated Occupational Safety and Health management system. That means combining isolated activities into a single system of targeted actions at all levels and stages of the production process.

Occupational safety is a system of legislative, socio-economic, organizational, technological, hygienic and therapeutic and prophylactic measures and tools that ensure the safety, preservation of health and human performance in the work process [92].

According to the Labor Code of the Russian Federation, every employee has the right:

- to have a workplace that meets Occupational safety requirements;
- to have a compulsory social insurance against accidents at manufacturing and occupational diseases;
- to receive reliable information from the employer, relevant government bodies and public organizations on conditions and Occupational safety at the workplace, about the existing risk of damage to health, as well as measures to protect against harmful and (or) hazardous factors;

– to refuse carrying out work in case of danger to his life and health due to violation of Occupational safety requirements;
– be provided with personal and collective protective equipment in compliance with Occupational safety requirements at the expense of the employer;
– for training in safe work methods and techniques at the expense of the employer;
– for personal participation or participation through their representatives in consideration of issues related to ensuring safe working conditions in his workplace, and in the investigation of the accident with him at work or occupational disease;
– for extraordinary medical examination in accordance with medical recommendations with preservation of his place of work (position) and secondary earnings during the passage of the specified medical examination;
– for warranties and compensation established in accordance with this Code, collective agreement, agreement, local regulatory an act, an employment contract, if he is engaged in work with harmful and (or) hazardous working conditions.

The labor code of the Russian Federation states that normal working hours may not exceed 40 hours per week, The employer must keep track of the time worked by each employee.

Rules for labor protection and safety measures are introduced in order to prevent accidents, ensure safe working conditions for workers and are mandatory for workers, managers, engineers and technicians.

4.3 Basic ergonomic requirements for the correct location and arrangement of researcher's workplace

The workplace when working with a PC should be at least 6 square meters. The legroom should correspond to the following parameters: the legroom height is at least 600 mm, the seat distance to the lower edge of the working surface is at least 150 mm,

and the seat height is 420 mm. It is worth noting that the height of the table should depend on the growth of the operator.

The following requirements are also provided for the organization of the workplace of the PC user: The design of the working chair should ensure the maintenance of a rational working posture while working on the PC and allow the posture to be changed in order to reduce the static tension of the neck and shoulder muscles and back to prevent the development of fatigue.

The type of working chair should be selected taking into account the growth of the user, the nature and duration of work with the PC. The working chair should be lifting and swivel, adjustable in height and angle of inclination of the seat and back, as well as the distance of the back from the front edge of the seat, while the adjustment of each parameter should be independent, easy to carry out and have a secure fit.

4.4 Occupational safety

A dangerous factor or industrial hazard is a factor whose impact under certain conditions leads to trauma or other sudden, severe deterioration of health of the worker.

A harmful factor or industrial health hazard is a factor, the effect of which on a worker under certain conditions leads to a disease or a decrease in working capacity.

4.4.1 Analysis of harmful and dangerous factors that can create object of investigation

During PET scanning the radiopharmaceuticals are implemented. As this drugs have radioactive isotopes all corresponding harmful and dangerous factors such as:

– Internal exposure to ionizing radiation occurs when radionuclides are inhaled, absorbed or otherwise entered the circulation.

– External radioactive contamination can occur when radioactive material in the air (dust, liquid, aerosols) settles on the skin or clothes.

– External irradiation of human body from different gamma – sources, also lead to DNA damage.

4.4.2 Analysis of harmful and dangerous factors that can arise at workplace during investigation

The working conditions in the workplace are characterized by the presence of hazardous and harmful factors, which are classified by groups of elements: physical, chemical, biological, psychophysiological. The main elements of the production process that form dangerous and harmful factors are presented in Table 4.1.

Table 4.1 – Possible hazardous and harmful factors

Factors (GOST 12.0.003-2015)	Work stages			Legal documents
	Development	Manufacture	Exploitation	
1. Deviation of microclimate indicators	+	+	+	Sanitary rules 2.2.2 / 2.4.1340–03. Sanitary and epidemiological rules and regulations "Hygienic requirements for personal electronic computers and work organization." Sanitary rules 2.2.1 / 2.1.1.1278–03. Hygienic requirements for natural, artificial and combined lighting of residential and public buildings. Sanitary rules 2.2.4 / 2.1.8.562–96. Noise at workplaces, in premises of residential, public buildings and in the construction area. Sanitary rules 2.2.4.548–96. Hygienic requirements for the microclimate of industrial premises.
2. Excessive noise		+	+	
3.Increased level of electromagnetic radiation	+	+	+	
4.Insufficient illumination of the working area		+	+	

5. Abnormally high voltage value in the circuit, the closure which may occur through the human body	+	+	+	Sanitary rules GOST 12.1.038-82 SSBT. Electrical safety. Maximum permissible levels of touch voltages and currents.

The following factors effect on person working on a computer:

– physical:

- temperature and humidity;
- noise;
- static electricity;
- electromagnetic field of low purity;
- illumination;
- presence of radiation;

– psychophysiological:

- physical overload (static, dynamic)
- mental stress (mental overstrain, monotony of work, emotional overload).

Deviation of microclimate indicators

The air of the working area (microclimate) is determined by the following parameters: temperature, relative humidity, air speed. The optimum and permissible values of the microclimate characteristics are established in accordance with [93] and are given in Table 4.2.

Table 4.2 – Optimal and permissible parameters of the microclimate

Period of the year	Temperature, C	Relative humidity,%	Speed of air movement, m/s
Cold and changing of seasons	23-25	40-60	0.1
Warm	23-25	40	0.1

Excessive noise

Noise and vibration worsen working conditions, have a harmful effect on the human body, namely, the organs of hearing and the whole body through the central nervous system. It result in weakened attention, deteriorated memory, decreased response, and increased number of errors in work. Noise can be generated by operating equipment, air conditioning units, daylight illuminating devices, as well as spread from the outside. When working on a PC, the noise level in the workplace should not exceed 50 dB.

Increased level of electromagnetic radiation

The screen and system blocks produce electromagnetic radiation. Its main part comes from the system unit and the video cable. According to [93], the intensity of the electromagnetic field at a distance of 50 cm around the screen along the electrical component should be no more than:

– in the frequency range 5 Hz - 2 kHz - 25 V / m;

– in the frequency range 2 kHz - 400 kHz - 2.5 V / m.

The magnetic flux density should be no more than:

– in the frequency range 5 Hz - 2 kHz - 250 nT;

– in the frequency range 2 kHz - 400 kHz - 25 nT.

Abnormally high voltage value in the circuit

Depending on the conditions in the room, the risk of electric shock to a person increases or decreases. Do not operate the electronic device in conditions of high humidity (relative air humidity exceeds 75% for a long time), high temperature (more than 35 ° C), the presence of conductive dust, conductive floors and the possibility of simultaneous contact with metal components connected to the ground and the metal casing of electrical equipment. The operator works with electrical devices: a computer (display, system unit, etc.) and peripheral devices. There is a risk of electric shock in the following cases:

– with direct contact with current-carrying parts during computer repair;

– when touched by non-live parts that are under voltage (in case of violation of insulation of current-carrying parts of the computer);
– when touched with the floor, walls that are under voltage;
– short-circuited in high-voltage units: power supply and display unit.

Table 4.3 – Upper limits for values of contact current and voltage

	Voltage, V	Current, mA
Alternate, 50 Hz	2	0.3
Alternate, 400 Hz	3	0.4
Direct	8	1.0

Insufficient illumination of the working area

Light sources can be both natural and artificial. The natural source of the light in the room is the sun, artificial light are lamps. With long work in low illumination conditions and in violation of other parameters of the illumination, visual perception decreases, myopia, eye disease develops, and headaches appear.

According to the standard, the illumination on the table surface in the area of the working document should be 300-500 lux. Lighting should not create glare on the surface of the monitor. Illumination of the monitor surface should not be more than 300 lux.

The brightness of the lamps of common light in the area with radiation angles from 50 to 90° should be no more than 200 cd/m, the protective angle of the lamps should be at least 40°. The safety factor for lamps of common light should be assumed to be 1.4. The ripple coefficient should not exceed 5%.

4.4.3 Justification of measures to reduce the levels of exposure to hazardous and harmful factors on the researcher

Deviation of microclimate indicators

The measures for improving the air environment in the production room

include: the correct organization of ventilation and air conditioning, heating of room. Ventilation can be realized naturally and mechanically. In the room, the following volumes of outside air must be delivered:

– at least 30 m^3 per hour per person for the volume of the room up to 20 m^3 per person;
– natural ventilation is allowed for the volume of the room more than 40 m^3 per person and if there is no emission of harmful substances.

The heating system must provide sufficient, constant and uniform heating of the air. Water heating should be used in rooms with increased requirements for clean air.

The parameters of the microclimate in the laboratory regulated by the central heating system, have the following values: humidity 40%, air speed 0.1 m/s, summer temperature 20-25 ° C, in winter 13-15 ° C. Natural ventilation is provided in the laboratory. Air enters and leaves through the cracks, windows, doors. The main disadvantage of such ventilation is that the fresh air enters the room without preliminary cleaning and heating.

Excessive noise

In research audiences, there are various kinds of noises that are generated by both internal and external noise sources. The internal sources of noise are working equipment, personal computer, printer, ventilation system, as well as computer equipment of other engineers in the audience. If the maximum permissible conditions are exceeded, it is sufficient to use sound-absorbing materials in the room (sound-absorbing wall and ceiling cladding, window curtains). To reduce the noise penetrating outside the premises, install seals around the perimeter of the doors and windows.

Increased level of electromagnetic radiation

There are the following ways to protect against EMF:

– increase the distance from the source (the screen should be at least 50 cm from the user);

– the use of pre-screen filters, special screens and other personal protective equipment.

When working with a computer, the ionizing radiation source is a display. Under the influence of ionizing radiation in the body, there may be a violation of normal blood coagulability, an increase in the fragility of blood vessels, a decrease in immunity, etc. The dose of irradiation at a distance of 20 cm to the display is 50 μrem/hr. According to the norms [93], the design of the computer should provide the power of the exposure dose of x-rays at any point at a distance of 0.05 m from the screen no more than 100 μR/h.

Fatigue of the organs of vision can be associated with both insufficient illumination and excessive illumination, as well as with the wrong direction of light.

Abnormally high voltage value in the circuit

Measures to ensure the electrical safety of electrical installations:

– disconnection of voltage from live parts, on which or near to which work will be carried out, and taking measures to ensure the impossibility of applying voltage to the workplace;
– posting of posters indicating the place of work;
– electrical grounding of the housings of all installations through a neutral wire;
– coating of metal surfaces of tools with reliable insulation;
– inaccessibility of current-carrying parts of equipment (the conclusion in the case of electroporating elements, the conclusion in the body of current-carrying parts) [94].

Insufficient illumination of the working area

Desktops should be placed in such a way that the monitors are oriented sideways to the light openings, so that natural light falls mainly on the left.

Also, as a means of protection to minimize the impact of the factor, local lighting should be installed due to insufficient lighting, window openings should be

equipped with adjustable devices such as blinds, curtains, external visors, etc.

4.5 Ecological safety

4.5.1 Analysis of the impact of the research object on the environment

Sources of ionizing radiation used in medicine could be divided into two groups: radioactive substances and radiation generators. The difference is that radiation generators like accelerators and x-ray tubes emit ionizing radiation only when they are turned on.

In ordinary work with necessary safety precautions, there are insignificant impact of using sources of ionizing radiation on environment. The immediate effect of ionizing radiation is ionization of air in room, but after a specified time the ionization disappears.

The danger of using radioactive materials could occur only in accidents with stealing and loosing these materials due to high toxicity.

4.5.2 Analysis of the environmental impact of the research process

Process of investigation itself in the thesis do not have essential effect on environment. One of hazardous waste is fluorescent lamps. Mercury in fluorescent lamps is a hazardous substance and its improper disposal greatly poisons the environment.

Outdated devices goes to an enterprise that has the right to process wastes. It is possible to isolate precious metals with a purity in the range of 99.95–99.99% from computer components. A closed production cycle consists of the following stages: primary sorting of equipment; the allocation of precious, ferrous and non-ferrous metals and other materials; melting; refining and processing of metals. Thus, there is an effective disposal of computer devices.

4.5.3 Justification of environmental protection measures

Pollution reduction is possible due to the improvement of devices that produces electricity, the use of more economical and efficient technologies, the use of new methods for generating electricity and the introduction of modern methods and methods for cleaning and neutralizing industrial waste. In addition, this problem should be solved by efficient and economical use of electricity by consumers themselves. This is the use of more economical devices, as well as efficient regimes of these devices. This also includes compliance with production discipline in the framework of the proper use of electricity.

Simple conclusion is that it is necessary to strive to reduce energy consumption, to develop and implement systems with low energy consumption. In modern computers, modes with reduced power consumption during long-term idle are widely used.

4.6 Safety in emergency

4.6.1 Analysis of probable emergencies that may occur at the workplace during research

The fire is the most probable emergency in our life. Possible causes of fire:

- malfunction of current-carrying parts of installations;
- work with open electrical equipment;
- short circuits in the power supply;
- non-compliance with fire safety regulations;
- presence of combustible components: documents, doors, tables, cable insulation, etc.

Activities on fire prevention are divided into: organizational, technical, operational and regime.

4.6.2 Substantiation of measures for the prevention of emergencies and the development of procedures in case of emergencies

Organizational measures provide for correct operation of equipment, proper maintenance of buildings and territories, fire instruction for workers and employees, training of production personnel for fire safety rules, issuing instructions, posters, and the existence of an evacuation plan.

The technical measures include compliance with fire regulations, norms for the design of buildings, the installation of electrical wires and equipment, heating, ventilation, lighting, the correct placement of equipment.

The regime measures include the establishment of rules for the organization of work, and compliance with fire-fighting measures. To prevent fire from short circuits, overloads, etc., the following fire safety rules must be observed:

- elimination of the formation of a flammable environment (sealing equipment, control of the air, working and emergency ventilation);
- use in the construction and decoration of buildings of non-combustible or difficultly combustible materials;
- the correct operation of the equipment (proper inclusion of equipment in the electrical supply network, monitoring of heating equipment);
- correct maintenance of buildings and territories (exclusion of the source of ignition - prevention of spontaneous combustion of substances, restriction of fire works);
- training of production personnel in fire safety rules;
- the publication of instructions, posters, the existence of an evacuation plan;
- compliance with fire regulations, norms in the design of buildings, in the organization of electrical wires and equipment, heating, ventilation, lighting;
- the correct placement of equipment;
- well-time preventive inspection, repair and testing of equipment.

In the case of an emergency, it is necessary to:

- inform the management (duty officer);

– call the Emergency Service or the Ministry of Emergency Situations - tel. 112;
– take measures to eliminate the accident in accordance with the instructions.

4.7 Conclusion

In this section about social responsibility the hazardous and harmful factors were revealed. All necessary safety measures and precaution to minimize probability of accidents and traumas during investigation are given.

Possible negative effect on environment were given in compact form describing main ecological problem of using nuclear energy.

It could be stated that with respect to all regulations and standards, investigation itself and object of investigation do not pose special risks to personnel, other equipment and environment.

Conclusion

Firstly, the existing commercially available small-animal PET scanners were observed. Most important characteristics such as: spatial resolution, energy resolution, sensitivity, axial and transaxial FOV were evaluated. Changing of parameters from older to state-of-art scanners shows main trends: increasing of axial FOV, decreasing of transaxial FOV, achievement of spatial resolution under 1 mm. Based on this main features of simulated scanner were determined: scintillator material is LYSO; ability of DOI evaluation through monolithic scintillator; electronic is d-SiPM. SiPM's are presented as checkboarded pattern with sensitive cell size 6x6 mm. The length of one unit of detector is 96 mm and width is 48. The thickness of scintillator is 24 mm that is doubled attenuation length for 511 keV photons.

Secondly, the unit of detector was simulated. Main physical electromagnetic and optical processes were determined. Cross-sections and deposition curves correspond to classical shapes for such experiments. Based on technical documentation the optical properties of scintillator were implemented for calculations. Explanation of degradation of energy resolution due to LYSO emission spectrum is given.

Finally, some performance characteristics of detector's unit were measured. Individual simulations show significant influence of distance between scatterings and XY determination error. However, evaluated maximum distance under 1 mm have around 40 % of all events. After this XY error determination was calculated an results show that generally 70 % of all events were determined with error less then 1 mm.

In this work were no covered also interesting questions such as: DOI performance calculation, increasing of spatial resolution near to edge of units and influence of coating on performance.

In future, it plans to provide full PET scanners model with evaluated performance on NEMA-4 2008 standard

List of student publications

Conference papers:

1. Gogolev, A.S. Development of software and hardware for tomographic examinations / A.S. Gogolev, N. A. Filatov, S. G. Chistyakov, N.V. Alekseev // Oilfield chemistry. Materials of the VII International Scientific and Practical Conference (XV All-Russian Scientific and Practical Conference). – Moscow: Russian State University of Oil and Gas (NRU) named after I.M. Gubkina. – 2020. – P. 179.

2. Bedenko, S. Thermo-physical properties of dispersion nuclear fuel for a new-generation reactors: A computational approach / S. Bedenko, A. Karengin, N. Ghal-Eh, N. Alekseev [at el.] // AIP Conference Proceedings. – 2019. – № 020002. – PP. 7. – DOI: 10.1063/1.5099594.

Theses:

1. Filatov, N.A. Development of the statistical methods for x-ray detector characterization to use in CT / N.A. Filatov, A.S. Gogolev, S.G. Chistyakov, N.V. Alekseev // Isotopes: technologies, materials and application collection of abstracts of the VI International scientific conference of young scientists, graduate students and students, Tomsk, October 26-29, 2020. – National Research Tomsk Polytechnic University (TPU). – 2020. – PP. 107-108.

2. Chistyakov, S.G. Development of a method for determining organochlorine compounds in a stream of oil / S. G. Chistyakov, N. A. Filatov, A. S. Gogolev, N. V. Alekseev // Isotopes: technologies, materials and application collection of abstracts of the VI International scientific conference of young scientists, graduate students and students, Tomsk, October 26-29, 2020. – National Research Tomsk Polytechnic University (TPU). – 2020. – PP. 108-109.

3. Alekseev, N.V. Computer modeling of the properties of nuclear fuel with a complex multicomponent structure / N.V. Alekseev, S. V. Bedenko, V. V. Knyshev [et al.] // Modern problems of physics and technology: a collection of abstracts of the VIII International Youth Scientific School-Conference: in 2 volumes. – 2019. – PP. 69-70.

4. Knyshev, V.V. Investigation of thermal and neutron load on micro-fuel coatings during long-term operation / V. V. Knyshev, N.V. Alekseev, A. I. Zorkin [et al.] // Modern problems of physics and technology: a collection of abstracts of the VIII International Youth Scientific School-Conference: in 2 volumes. – 2019. – P. 128.

5. Kuznetsova, M.E. Calculated assessment of the thermal conductivity of heterogeneous nuclear fuel / M.E. Kuznetsova, N.V. Alekseev, S.V. Bedenko // Modern problems of physics and technology: a collection of abstracts of the VIII International Youth Scientific School-Conference: in 2 volumes. – 2019. – P. 128.

6. Alekseev, N.V. Features of dispersion nuclear fuel radiation with complex inertial structure / N.V. Alekseev, R. Sabitova, M.E. Kuznetsova // Lomonosov - 2019. Section "Physics": a collection of abstracts of the XXVI International conference of students, graduate students and young scientists in fundamental sciences. – Moscow. – April 8-12, 2019. – Moscow: Moscow State University. – P.P. 58-59.

7. Alekseev, N.V. Investigation of the properties of nuclear fuel with a complex internal structure for fission and fusion reactors: computer simulation / N.V. Alekseev, S.V. Bedenko, O.A. Ukrainets // Lomonosov - 2019. Section "Physics": collection of abstracts of the XXVI International conference students, graduate students and young scientists in fundamental sciences. – Moscow. – 2019. - Moscow: Moscow State University. – PP. 113-114.

8. Alekseev, N.V. Features of the spatial kinetics of a hybrid thorium reactor facility with an extended plasma neutron source based on a magnetic trap / N.V. Alekseev, I.O Lutsik, V.V. Knyshev [et al.] // Lomonosov - 2019. Section "Physics": collection of abstracts of the XXVI International conference students, graduate students and young scientists in fundamental sciences. – Moscow. – 2019. - Moscow: Moscow State University. – P. 87.

9. Knyshev, V.V. Changes in the thermophysical properties of micro-fuel coatings under the influence of neutron radiation and fission products / V.V. Knyshev, N.V. Alekseev, Kuznetsova M.E. [et al.] // Lomonosov - 2019. Section "Physics": collection of abstracts of the XXVI International conference students, graduate students and young scientists in fundamental sciences. – Moscow. – 2019. - Moscow:

Moscow State University. – PP. 81-82.

10. Shamanin, I.V. Spatial distribution of temperature in the fuel compact of a high-temperature reactor installation // I.V. Shamanin, A.G. Karengin, V.V. Knyshev [et al.] // IX School-Conference young nuclear scientists of Siberia: collection of abstracts, Tomsk, 17-19 October 2018. – Tomsk: Hang-glider. – 2018. – P. 54.

References

1. Schlyer, D. J. PET tracers and radiochemistry / D. J. Schlyer // Annals of the Academy of Medicine. – 2004. –Vol. 33, № 2. – PP. 146-154.

2. Britannica, The Editors of Encyclopaedia. "Cyclotron". Encyclopedia Britannica: site. – 8 Feb. 2018. – URL: https://www.britannica.com/technology/cyclotron (Accessed 6 June 2021). – Text: electronic.

3. Saha, G. B. Basics of PET Imaging / G. B. Saha; Springer International Publishing. – Switzerland, 2016. – 282 pp. – ISBN 978-3-319-16422-9

4. Rensch, C. Microfluidics: a groundbreaking technology for PET tracer production? / C. Rensch, A. Jackson, S. Lindner [et al.] // Molecules. – 2013. – Vol.18, №7. – PP. 7930-7956. – DOI: 10.3390/molecules18077930.

5. Guerra, A. D. Ionizing Radiation Detectors for Medical Imaging / A. D. Guerra; World Scientific. – Italy, 2004. – 524 pp. – ISBN: 978-981-4483-73-5.

6. Cherry, S.R. Use of positron emission tomography in animal research / S. R. Cherry, S. S. Gambhir // ILAR J. – 2001. – Vol.42, № 3. – PP. 219 – 232. – DOI: 10.1093/ilar.42.3.219.

7. Tong, S. Image reconstruction for PET/CT scanners: past achievements and future challenges / S. Tong, A. M. Alessio, P. E. Kinahan // Imaging in medicine. – 2010. – Vol. 2, № 5. – PP. 529-545. – DOI: 10.2217/iim.10.49.

8. Brinks, R. Image reconstruction in positron emission tomography (PET): the 90th anniversary of Radon's solution / R. Brinks, T. M. Buzug // Biomedical Engineering. – 2007. – Vol. 52, № 6. – PP. 361-364. – DOI: 10.1515/BMT.2007.060.

9. Schofield, R. Image reconstruction: Part 1 – understanding filtered back projection, noise and image acquisition / R. Schofield, L. King, U. Tayal [et al.] // Journal of Cardiovascular Computed Tomography. – 2019. – Vol. 14, № 3. – PP. 219-225. – DOI: 10.1016/j.jcct.2019.04.008.

10. Zeng, G. L. Revisit of the Ramp Filter / G. L. Zeng // IEEE Transactions on Nuclear Science. – 2015. – Vol.61, № 1. – PP. 131-136. – DOI: 10.1109/TNS.2014.2363776.

11. Ramachandran, G. N. Three-dimensional reconstruction from radiographs and electron micrographs: application of convolutions instead of Fourier transforms / G. N. Ramachandran, A. V. Lakshminarayanan // Proceedings of the National Academy of Sciences of the United States of America. – 1971. – Vol. 68, № 9. – PP. 2236-2240. – DOI: 10.1073/pnas.68.9.2236.

12. Lyra, M. Filtering in SPECT Image Reconstruction / M. Lyra, A. Ploussi // International Journal of Biomedical Imaging. – 2011. – Vol. 2011, № 693795. – PP. 14. – DOI: 10.1155/2011/693795.

13. Shepp, L. A. The Fourier reconstruction of a head section / L. A. Shepp, B. F. Logan // IEEE Transactions on Nuclear Science. – 1974. – Vol. 21, № 3. – PP. 21-43. – DOI: 10.1109/TNS.1974.6499235.

14. Shepp, L. A. Maximum Likelihood Reconstruction for Emission Tomography / L. A. Shepp, Y. Vardi // IEEE Transactions on Medical Imaging. – 1982. – Vol. 1, № 2. – PP. 113-122. – DOI: 10.1109/TMI.1982.4307558.

15. Gaitanis, A. PET image reconstruction: A stopping rule for the MLEM algorithm based on properties of the updating coefficients / A. Gaitanis, G. Kontaxakis, G. Spyrou [et al.] // Computerized Medical Imaging and Graphics : the Official Journal of the Computerized Medical Imaging Society. – 2009. – Vol. 34, № 2. – PP. 131-141. – DOI: 10.1016/j.compmedimag.2009.07.006.

16. Hudson, H. M. Accelerated image reconstruction using ordered subsets of projection data / H. M. Hudson, R. S. Larkin // IEEE transactions on medical imaging. – 1994. – Vol. 13, № 4. – PP. 601-609. – DOI: 10.1109/42.363108.

17. Gordon, R. Algebraic Reconstruction Techniques (ART) for three-dimensional electron microscopy and X-ray photography / R. Gordon, R. Bender, G. T. Herman // Journal of Theoretical Biology. – 1970. – Vol. 29, № 3. – PP. 471-481. – DOI: 10.1016/0022-5193(70)90109-8.

18. El Moataz, A. Image and Signal Processing // A. El Moataz, D. Mammass, A. Mansouri [et al.] // Lecture Notes in Computer Science. –2016. – Vol. 9680. – PP. 388.

19. Andersen, A. Simultaneous Algebraic Reconstruction Technique (SART):

A superior implementation of the ART algorithm / A. Andersen // Ultrasonic Imaging. – 1984. – Vol. 6, № 1. – PP: 81-94. – DOI: 10.1016/0161-7346(84)90008-7.

20. Boudjelal, A. Improved Simultaneous Algebraic Reconstruction Technique Algorithm for Positron-Emission Tomography Image Reconstruction via Minimizing the Fast Total Variation / A. Boudjelal, Z. Messali, A. Elmoataz [et al.] // Journal of Medical Imaging and Radiation Sciences. – 2017. – Vol. 48, № 4. – PP. 385-393. – DOI: 10.1016/j.jmir.2017.09.005.

21. Levitan, E. A Maximum a Posteriori Probability Expectation Maximization Algorithm for Image Reconstruction in Emission Tomography / E. Levitan, G. T. Herman // IEEE Transactions on Medical Imaging. – 1987. – Vol. 6, № 3. – PP. 185-192. – DOI: 10.1109/TMI.1987.4307826.

22. Zhou, J. A Bayesian MAP-EM Algorithm for PET Image Reconstruction Using Wavelet Transform // J. Zhou, J.-L. Coatrieux, A. Bousse [et al.] // IEEE Transactions on Nuclear Science. – 2007. – Vol. 54, № 5. – PP. 1660-1669. – DOI: 10.1109/TNS.2007.901200.

23. Green, P. J. Bayesian reconstructions from emission tomography data using a modified EM algorithm / P. J. Green // IEEE Transactions on Medical Imaging. – 1990. – Vol. 9, № 1. – PP. 84-93. – DOI: 10.1109/42.52985

24. Bettinardi, V. Implementation and evaluation of a 3D one-step late reconstruction algorithm for 3D positron emission tomography brain studies using median root prior / V. Bettinardi, E. Pagani, M. Gilardi [et al.] // European Journal of Nuclear Medicine and Molecular Imaging. – 2002. – Vol. 29, № 1. – PP. 7-18. – DOI: 10.1007/ s002590100651.

25. D'Ambrosio, D. Attenuation Correction for Small Animal PET Images: A Comparison of Two Methods / D. D'Ambrosio, F. Zagni, A. E. Spinelli [et al.] // Computational and Mathematical Methods in Medicine. – 2013. – Vol. 2013. – PP. 1-12. – DOI: 10.1155/2013/103476.

26. Ollinger, J. M. Model-based scatter correction for fully 3D PET / J. M. Ollinger // Physics in Medicine and Biology. – 1996. – Vol. 41, № 1. – PP. 153-176. – DOI: 10.1088/0031-9155/41/1/012.

27. Holdsworth, C. H. Investigation of accelerated Monte Carlo techniques for PET simulation and 3D PET scatter correction / C. H. Holdsworth, C.S. Levin, T. H. Farquhar [et al.] // IEEE Transactions on Nuclear Science. – 2001. – Vol. 48, № 1. – PP. 74-81. – DOI: 10.1109/23.910835.

28. Brasse, D. Correction methods for random coincidences in fully 3D whole-body PET: impact on data and image quality / D. Brasse, P. E. Kinahan, C. Lartizien [et al.] // Journal of nuclear medicine. – 2005. – Vol. 46, № 5. – PP. 859-867. – PMID: 15872361.

29. Hoffman, E. J. PET system calibrations and corrections for quantitative and spatially accurate images / E. J. Hoffman, T. M. Guerrero, G. Germano [et al.] // IEEE Transactions on Nuclear Science. – 1989. – Vol. 36, № 1. – PP. 1108-1112. – DOI: 10.1109/23.34613.

30. Kinahan, P. E. Efficiency normalization techniques for 3D PET data / P. E. Kinahan, D. W. Townsend, D. L. Bailey [et al.] // IEEE Nuclear Science Symposium and Medical Imaging Conference Record. – 1995. – DOI: 10.1109/NSSMIC.1995. 510439.

31. Germano, G. Investigation of Count Rate and Deadtime Characteristics of a High Resolution PET System / G. Germano, E. J. Hoffman // Journal of Computer Assisted Tomography. – 1988. – Vol. 12, № 5. – PP. 836-846.

32. Ter-Pogossian, M. M. Super PETT I: A Positron Emission Tomograph Utilizing Photon Time-of-Flight Information / M. M. Ter-Pogossian, D. C. Ficke, M. Yamamoto [et al.] // IEEE Transactions on Medical Imaging. – 1982. – Vol. 1, № 3. – PP. 179-187. – DOI: 10.1109/TMI.1982.4307570.

33. Surti, S. Update on Time-of-Flight PET Imaging / S. Surti // Journal of Nuclear Medicine. – 2014. – Vol. 56, № 1. – PP. 98-105. – DOI: 10.2967/jnumed. 114.145029.

34. DiFilippo F. P. Small-animal imaging using clinical positron emission tomography/computed tomography and super-resolution / F. P. DiFilippo, S. Patel, K. Asosingh [et al.] // Molecular imaging. – 2012. – Vol. 11, № 3. – PP. 210-219. – PMID: 22554485.

35. Performance Measurements of Small Animal Positron Emission Tomographs (PETs): site. – URL: https://www.nema.org/standards/view/Performance-Measurements-of-Small-Animal-Positron-Emission-Tomographs (Accessed 6 June 2021).

36. Goertzen, A. L. NEMA NU 4-2008 Comparison of Preclinical PET Imaging Systems / A. L. Goertzen, Q. Bao, M. Bergeron [et al.] // Journal of Nuclear Medicine. – 2012. – Vol. 53, № 8. – PP. 1300-1309. – DOI: 10.2967/jnumed.111.099382.

37. Yao, R. Small-Animal PET: What Is It, and Why Do We Need It? / R. Yao, R. Lecomte, E.S. Crawford // Journal of Nuclear Medicine Technology. – 2012. – Vol. 40, № 3. – PP. 157-165. – DOI: 10.2967/jnmt.111.098632.

38. Larobina, M. Small Animal PET: A Review of Commercially Available Imaging Systems / M. Larobina, A. Brunetti, M. Salvatore // Current Medical Imaging Reviews. – 2006. – Vol. 2, № 2. – PP. 187-192. – DOI: 10.2174/157340506776930610.

39. Amirrashedi, M. Advances in Preclinical PET Instrumentation / M. Amirrashedi, H. Zaidi, M. R. Ay // PET Clinics. – 2020. – Vol. 15, № 4. – PP. 403-426. – DOI: 10.1016/j.cpet.2020.06.003.

40. Gonzalez, A. J. Next generation of the Albira small animal PET based on high density SiPM arrays / A. J. Gonzalez, A. Aguilar, P. Conde [et al.] // 2015 IEEE Nuclear Science Symposium and Medical Imaging Conference. – 2015. PP. 4. – DOI: 10.1109/NSSMIC.2015.7582085.

41. Gu, Z. Performance evaluation of G8, a high sensitivity benchtop preclinical PET/CT tomograph / Z. Gu, R. Taschereau, N. Vu [et al.]// Journal of Nuclear Medicine. – 2018. – Vol. 60, № 1. – PP. 142-149. – DOI: 10.2967/jnumed.118.208827.

42. Gu, Z. NEMA NU-4 performance evaluation of PETbox4, a high sensitivity dedicated PET preclinical tomograph / Z. Gu, R. Taschereau, N. Vu [et al.] // Physics in Medicine and Biology. – 2013. – Vol. 58, № 11. – PP. 3791-3814. – DOI: 10.1088/0031-9155/58/11/3791.

43. Krishnamoorthy, S. Performance evaluation of the MOLECUBES β-

CUBE—a high spatial resolution and high sensitivity small animal PET scanner utilizing monolithic LYSO scintillation detectors / S. Krishnamoorthy, E. Blankemeyer, P. Mollet [et al.] // Physics in Medicine & Biology. – 2018. – Vol. 63, № 15. – DOI: 10.1088/1361-6560/aacec3.

44. Chai, P. NEMA NU-4 performance evaluation of a non-human primate animal PET / P. Chai, B. Feng, Z. Zhang [et al.] // Physics in Medicine and Biology. – 2019. – Vol. 64, № 10. – DOI: 10.1088/1361-6560/ab1614.

45. Canadas, M. NEMA NU 4-2008 Performance Measurements of Two Commercial Small-Animal PET Scanners: ClearPET and rPET-1 / M. Canadas, M. Embid, E. Lage [et al.] // IEEE Transactions on Nuclear Science. – 2011. – Vol. 58, № 1. – PP. 58-65. – DOI: 10.1109/TNS.2010.2072935.

46. Bergeron, M. Performance evaluation of the LabPET12, a large axial FOV APD-based digital PET scanner / M. Bergeron, J. Cadorette, C. Bureau-Oxton [et al.] // 2009 IEEE Nuclear Science Symposium Conference Record. – 2009. – DOI: 10.1109/NSSMIC.2009.5401915.

47. Sato, K. Performance evaluation of the small-animal PET scanner ClairvivoPET using NEMA NU 4-2008 Standards / K. Sato, M. Shidahara, H. Watabe [et al.] // Physics in Medicine and Biology. – 2015. – Vol. 61, № 2. – PP. 696-711. – DOI: 10.1088/0031-9155/61/2/696.

48. Lage, E. VrPET/CT: Development of a rotating multimodality scanner for small-animal imaging / E. Lage, J. J. Vaquero, A. Sisniega [et al.] // 2008 IEEE Nuclear Science Symposium Conference Record. – 2008. – DOI: 10.1109/NSSMIC.2008. 4774465.

49. Goorden M. C. VECTor: a preclinical imaging system for simultaneous submillimeter SPECT and PET / M. C. Goorden, F. van der Have, R. Kreuger [et al] // Journal of nuclear medicine. – 2013. – Vol. 54, № 2. – PP. 306-312. – DOI: 10.2967/jnumed.112.109538.

50. Melcher, C. Scintillation crystal for PET / C. Melcher // Journal of nuclear medicine. – 2000. – Vol. 41, № 6. – PP. 1051-1055. – PMID: 10855634.

51. BGO Bismuth Germanate Scintillation Material / Saint-Gobain: site. –

URL: https://www.crystals.saint-gobain.com/sites/imdf.crystals.com/files/documents/bgo-material-data-sheet.pdf (Accessed 6 June 2021).

52. Zhang, H. Performance Characteristics of BGO Detectors for a Low Cost Preclinical PET Scanner / H. Zhang, N. T. Vu, Q. Bao [et al.] // IEEE Transactions on Nuclear Science. – 2010. – Vol. 57, № 3. – PP. 1038-1044. – DOI: 10.1109/TNS.2010.2046753.

53. LYSO Scintillation Material / Saint-Gobain: site. – URL: https://www.crystals.saint-gobain.com/sites/imdf.crystals.com/files/documents/lyso-material-data-sheet.pdf (Accessed 6 June 2021).

54. Pepin, C. M. Properties of LYSO and recent LSO scintillators for phoswich PET detectors / C. M. Pepin, P. Berard, A.-L. Perrot [et al.] // IEEE Transactions on Nuclear Science. – 2004. – Vol. 51, № 3. – PP. 789-795. – DOI: 10.1109/TNS.2004.829781.

55. Matulewicz T. Tests of GSO scintillator / T. Matulewicz, K. Korzecka, Z. Pytel // Internation Atomic Energy Agency. – 1996. – PP. 2. – URL: https://inis.iaea.org/collection/NCLCollectionStore/_Public/29/003/29003603.pdf

56. Yamamoto, S. A GSO depth of interaction detector for PET / S. Yamamoto, H. Ishibashi // IEEE Transactions on Nuclear Science. – 1998. – Vol. 45, № 3. – PP. 1078-1082. – DOI: 10.1109/23.681982.

57. Yamamoto, S. Possibility analysis of a GSO PET/SPECT detector / S. Yamamoto [et al.] // 2000 IEEE Nuclear Science Symposium. Conference Record. – 2000. – DOI: 10.1109/NSSMIC.2000.950016.

58. Nassalski, A. Comparative Study of Scintillators for PET/CT Detectors / A. Nassalski, M. Kapusta, T. Batsch [et al.] // IEEE Transactions on Nuclear Science. – 2007. – Vol. 54, № 1. – PP. 3-10. – DOI: 10.1109/tns.2006.890013.

59. Trummer, J. Scintillation Properties of LuYAP and LYSO Crystals Measured with MiniACCOS, an Automatic Crystal Quality Control System / J. Trummer, D. Aimard, E. Auffray [et al.] // IEEE Nuclear Science Symposium Conference Record, 2005. – 2005. – PP. 4. – DOI: 10.1109/NSSMIC.2005.1596918.

60. Jiang, W. Sensors for Positron Emission Tomography Applications / W

Jiang, Y. Chalich, M. J. Deen // Sensors. – 2019. – Vol. 19, № 22. – DOI: 10.3390/s19225019.

61. Soonseok K. High Resolution GSO Block Detectors Using PMT-Quadrant-Sharing Design for Small Animal PET / K. Soonseok, X. Shuping, R. Ramirez [et al.] // IEEE Symposium Conference Record Nuclear Science 2004. – 2004. – Vol. 6. – PP. 3385-3388. – DOI: 10.1109/NSSMIC.2004.1466613.

62. Shao, Y. Evaluation of multi-channel PMTs for readout of scintillator arrays / Y. Shao, S. R. Cherry, S. Siegel [et al.] // Nuclear Instruments and Methods in Physics Research Section A: Accelerators, Spectrometers, Detectors and Associated Equipment. – 1997. – Vol. 390, № 1-2. – PP. 209-218. – DOI: 10.1016/S0168-9002(97)00379-3.

63. Alva, H. Characterisation of a Position-Sensitive Photomultiplier Tube for MicroPET Detection Modules / H. Alva, M. Rodríguez-Villafuerte, A. Martínez-Dávalos [et al.] // AIP Conference Proceedings. – 2006. – Vol. 854, № 1. – PP. 42-44. – DOI: 10.1063/1.2356396.

64. Grazioso, R. APD-based PET detector for simultaneous PET/MR imaging / R. Grazioso, N. Zhang, J. Corbeil [et al.] // Nuclear Instruments and Methods in Physics Research Section A: Accelerators, Spectrometers, Detectors and Associated Equipment. – 2006. – Vol. 569, № 2. – PP. 301-305. – DOI: 10.1016/j.nima.2006.08.121.

65. Grazioso, R. APD performance in light sharing PET applications / R. Grazioso, M. Aykac, M. E.Casey [et al.] // IEEE Transactions on Nuclear Science. – 2005. – Vol. 52, № 5. – PP. 1413-1416. – DOI: 10.1109/TNS.2005.857628.

66. Roncali, E. Application of Silicon Photomultipliers to Positron Emission Tomography / E. Roncali, S. R. Cherry // Annals of Biomedical Engineering. – 2011. – Vol. 39, № 4. – PP. 1358-1377. – DOI: 10.1007/s10439-011-0266-9.

67. Gundacker, S. The silicon-photomultiplier: fundamentals and applications of a modern solid-state photon detector / S. Gundacker, A. Heering // Physics in Medicine & Biology. – 2020. – Vol. 65, № 17. – PP. 44. – DOI: 10.1088/1361-6560/ab7b2d.

68. A dedicated tool for PET scanner simulations using FLUKA: site. – URL: https://indico.cern.ch/event/260259/contributions/578223/attachments/459045/636105/OrtegaPG_FLUKAmeeting.pdf (Accessed 6 June 2021).

69. Ito, M. Progress in Nuclear Imaging / M. Ito. – 2011. – Seoul National University. – URL: https://slidetodoc.com/progress-in-nuclear-imaging-mikiko-ito-ph-d/.

70. Ito, M. Positron emission tomography (PET) detectors with depth-of-interaction (DOI) capability / M. Ito, S. J. Hong, J. S. Lee // Biomedical Engineering Letters. – 2011. – Vol. 1, № 2. – PP. 70-81. – DOI: 10.1007/s13534-011-0019-6.

71. Ito, M. A Four-Layer DOI Detector With a Relative Offset for Use in an Animal PET System / M. Ito, J.S. Lee, S. I. Kwon [et al.] // IEEE Transactions on Nuclear Science. – 2010. – Vol. 57, № 3. – PP. 976-981. – DOI: 10.1109/TNS.2010.2044892.

72. Rafecas, M. A Monte Carlo study of high-resolution PET with granulated dual-layer detectors / M. Rafecas, G. Boning, B. J. Pichler [et al.] // IEEE Transactions on Nuclear Science. – 2001. – Vol. 48, № 4. – PP. 1490-1495. – DOI: 10.1109/NSSMIC.2000.949301.

73. McElroy, D. P. A true singles list-mode data acquisition system for a small animal PET scanner with independent crystal readout / D. P. McElroy, M. Hoose, W. Pimpl [et al.] // Physics in Medicine and Biology. – 2005. – Vol. 50, № 14. – PP. 3323-3335. – DOI: 10.1088/0031-9155/50/14/009.

74. Seidel, J. Depth identification accuracy of a three layer phoswich PET detector module / J. Seidel, J. J. Vaquero, S. Siegel [et al.] // IEEE Transactions on Nuclear Science. – 1999. – Vol. 46, № 3. – PP. 485-490. – DOI: 10.1109/23.775567.

75. Yang, Y. Depth of interaction calibration for PET detectors with dual-ended readout by PSAPDs / Y. Yang, J. Qi, Y. Wu [et al.] // Physics in Medicine and Biology. – 2011. – Vol. 54, № 2. – PP. 433-445. – DOI: 10.1088/0031-9155/54/2/017.

76. Van Dam, H. T. Improved Nearest Neighbor Methods for Gamma Photon Interaction Position Determination in Monolithic Scintillator PET Detectors / H. T. Van Dam, S. Seifert, R. Vinke [et al.] // IEEE Transactions on Nuclear Science. – 2011.

– Vol. 58, № 5. – PP. 2139-2147. – DOI: 10.1109/TNS.2011.2150762.

77. Roncali, E. Design Considerations for DOI-encoding PET Detectors Using Phosphor-Coated Crystals / E. Roncali, V. Viswanath, S. R. Cherry // IEEE Transactions on Nuclear Science. – 2014. – Vol. 62, № 1. – PP. 67-73. – DOI: 10.1109/TNS.2013.2293313

78. Gendler D. Derivation of an Algorithm for Calculation of the Intesection Area of a Circle with a Grid with Finite Fill Factor / D. Gendler, C. Eisele, D. Seiffer [et al.] // Arxiv. – URL: https://arxiv.org/ftp/arxiv/papers/1812/1812.10515.pdf.

79. Gauss's Circle Problem / WolframMathWorld: site. – URL: https://mathworld.wolfram.com/GausssCircleProblem.html (Accessed 6 June 2021).

80. Allison, J. Geant4 developments and applications / J. Allison, K. Amako, J. Apostolakis [et al.] // IEEE Transactions on Nuclear Science. – 2006. – Vol. 53, № 1. – PP. 270-278. – DOI: 10.1109/TNS.2006.869826.

81. EM Opt4 / Geant4: site. – URL: https://geant4-userdoc.web.cern.ch/UsersGuides/PhysicsListGuide/html/electromagnetic/Opt4.html (Accessed 6 June 2021).

82. Brown, J. M. A low energy bound atomic electron Compton scattering model for Geant4 / J. M. C. Brown, M. R. Dimmock, J. E. Gillam [et al.] // Nuclear Instruments and Methods in Physics Research Section B: Beam Interactions with Materials and Atoms. – 2014. – Vol. 338. – PP. 77-88. – DOI: 10.1016/j.nimb.2014.07.042.

83. Ivanchenko, V. Progress of Geant4 electromagnetic physics developments and applications / V. Ivanchenko, A. Bagulya, S. Bakr [et al.] // EPJ Web of Conferences. – 2019. – Vol. 214, № 02046. – PP. 8. – DOI: 10.1051/epjconf/201921402046.

84. Kadri, O. Incorporation of the Goudsmit–Saunderson electron transport theory in the Geant4 Monte Carlo code / O. Kadri, V. Ivanchenko, F. Gharbi [et al.] // Nuclear Instruments and Methods in Physics Research Section B: Beam Interactions with Materials and Atoms. – 2009. – Vol. 267, № 23-24. – PP. 3624-2632. – DOI: 10.1016/j.nimb.2009.09.015.

85. J-Series SiPM Sensors / On Semiconductor: site. – URL: https://www.onsemi.com/pdf/datasheet/microj-series-d.pdf (Accessed 6 June 2021).

86. Gonzalez, A. J. A PET Design Based on SiPM and Monolithic LYSO Crystals: Performance Evaluation / A. J. Gonzalez, A. Aguilar, P. Conde [et al.] // IEEE Transactions on Nuclear Science. – 2016. – Vol. 63, № 4. – PP. 2471-2477. – DOI: 10.1109/TNS.2016.2522179.

87. Kuang, Z. Performance of a high-resolution depth encoding PET detector using barium sulfate reflector / Z .Kuang, X. Wang, C. Li [et al.] // Physics in Medicine & Biology. – 2017. – Vol. 62, № 15, - PP. 5945-5958. – DOI: 10.1088/1361-6560/aa71f3.

88. Physics Reference Manual / Geant4: site. – URL: https://geant4-userdoc.web.cern.ch/UsersGuides/PhysicsReferenceManual/html/index.html (Accessed 6 June 2021).

89. Yazaki Y. How the Klein–Nishina formula was derived: Based on the Sangokan Nishina Source Materials / Y. Yazaki // Proceedings of the Japan Academy, Series B. – 2017. – Vol. 93, № 6. – PP. 399-412. – DOI: 10.2183/pjab.93.025.

90. Bonifacio, D. A. B. Modeling of 3D gamma interaction position in a monolithic scintillator block with a row-column summing readout / D. A. Bonifacio, M. Moralles // 2012 IEEE Nuclear Science Symposium and Medical Imaging Conference Record. – 2012. – PP. 2606-2613. – DOI: 10.1109/NSSMIC.2012.6551596.

91. Borghi, G. Towards monolithic scintillator based TOF-PET systems: practical methods for detector calibration and operation / G. Broghi, V. Tabacchini, D. R. Schaart // Physics in Medicine and Biology. – 2016. – Vol. 61, № 13. – PP. 4904-4928. – DOI: 10.1088/0031-9155/61/13/4904.

92. GOST 12.2.032-78 Occupational safety standards system. Operator's location in a sitting position. General ergonomic requirements. Date of validity: 1979-01-01. – URL: https://docs.cntd.ru/document/1200003913 (Accessed 6 June 2021). – Text: electronic.

93. SR 2.4.3648-20 Sanitary and Epidemiological Requirements for

Organizations of Education and Training, Recreation and Recreation of Children and Youth. Date of validity: 2021-01-01. – URL: https://docs.cntd.ru/document/566085656?marker=6580IP (Accessed 6 June 2021). – Text: electronic.

94. GOST 12.1.038-82 Occupational safety standards system. Electrical safety. Date of validity: 1983-07-01. – URL: https://docs.cntd.ru/document/5200313 (Accessed 6 June 2021). – Text: electronic.

Appendix A

Table A.1 – Design characteristics of small-animal PET scanners

Scanner	Manufacturer	Scintillator	Cristal dimensions, mm^3	Electronic	Transaxial FOV, mm	Axial FOV, mm
microPET P4	Siemens	LSO (8 x 8)	2.2 x 2.2 x 10	PSPMT	190	78
microPET Focus-220	Siemens	LSO (12 x 12)	1.5 x 1.5 x 10	PSPMT	190	76
Inveon-DPET	Siemens	LSO (20 x 20)	1.5 x 1.5 x 10	PSPMT	100	127
Mosaic-HP	Philips	GSO	2 x 2 x 10	PMT	128	119
Argus	Sedecal	LYSO/GSO (13 x 13)/(20 x 20)	1.45 x 1.45 x 7/8	PSPMT	67	48
ClearPET	Raytest GmbH	LYSO/LuYAP (8 x 8)/(8 x 8)	2 x 2 x 10/10	PSPMT	144	110
VrPET	Sedecal	LYSO (30 x 30)	1.4 x 1.4 x 12	PSPMT	86.6	45.6
LabPET12	Gamma Medica	LYSO/LGSO	2 x 2 x 11.9/13.3	APD	100	112.5
X-PET	Gamma Medica	BGO (8 x 8)	2.3 x 2.3 x 9.4	PMT	100	116
NanoPET/CT	Mediso	LYSO (39 x 81)	1.1 x 1.1 x 13	PSPMT	123	94.8
nanoScan (PET82S)	Mediso	LYSO (29 x 29)	1.5 x 1.5 x 10	PSPMT	80	98.6
Albira	Bruker	LYSO (monolithic)	50 x 50 x 10	MAPMT	80	148
Albira Si	Bruker	LYSO (monolithic)	50 x 50 x 10	SiPM	80	148
PETbox4	UCLA	BGO (24 x 50)	1.8 x 1.8 x 7	PSPMT	45	95
G4	Sofie Bioscience	BGO (24 x 50)	1.8 x 1.8 x 7	MAPMT	45	94
G8	Sofie Bioscience	BGO (26 x 26)	1.8 x 1.8 x 7.2	MAPMT	47.44	94.95
GNEXT	Sofie Bioscience	LYSO/BGO (8 x 8)/(8 x 8)	1.01 x 1.01 x 6.1 1.5 x 1.5 x 8.9	Not available	120	104
ClairvivoPET	Shimadzu	LYSO/LYSO (32 x 53)/(32 x 54)	1.3 x 2.7 x 7	PMT	102	151

Scanner	Manufacturer	Scintillator	Cristal dimensions, mm^3	Electronic	Transaxial FOV, mm	Axial FOV, mm
TransPET-LH	Raycan	LYSO	1.9 x 1.9 x 13	PSPMT	130	53
Xtrim-PET	Parto Negar Persia	LYSO (24 x 24)	2.1 x 2.1 x 10	SiPMs	100	50.3
β-cubes	Molecubes	LYSO (monolithic)	25 x 25 x 8	MPPC	72	130
VECTor	MILabs	NaI(Tl) (monolithic)	590 x 470 x 9.5	Not available	48	36
MuPET	University of Texas M.D. Anderson Cancer Center	LYSO (30 x 30)	1.2 x 1.4 x 9.5	PMT	100	116

Table A.2 – Performance characteristics of small-animal PET scanners

Scanner	Spatial resolution, mm	Energy resolution, %	Peak absolute sensitivity, mm^3	Noise equivalent count rate-Mice, kcps	Scatter fraction, %
microPET P4	2.29 (at 5 mm)	26	1.19	601	5.2
microPET Focus-220	1.75 (at 5 mm)	18.5	2.06	763	7.2
Inveon-DPET	1.63 (at 5 mm)	14.6	3.42	1670	7.8
Mosaic-HP	2.70	17	2.28	555	5.4
Argus	1.63	26	6.72	117	21.0
ClearPET	1.94 (at 5 mm)	25	2.83	73	31.0
VrPET	1.48	16.5	2.22	74	11.5
LabPET12	1.65 (at 5 mm)	19	5.40	362	16.0
X-PET	2.00	Not available	9.30	106	7.9
NanoPET/CT	1.03	19	8.40	430	15.0
Albira	1.55	18	6.30	Not available	Not available
Albira Si	0.89	15	9.00	576	Not available
PETbox4	1.61	18	18.10	35	28.0
G4	1.35	18	14.00	Not available	Not available
G8	< 1.00	19.3	9.00	44	11.0
ClairvivoPET	2.16 (at 5 mm)	Not available	8.70	415	17.7

Scanner	Spatial resolution, mm	Energy resolution, %	Peak absolute sensitivity, mm^3	Noise equivalent count rate-Mice, kcps	Scatter fraction, %
TransPET-LH	0.95	13	2.40	110	11.0
Xtrim-PET	2.01	12	2.20	113	12.5
β-cubes	1.06	12	5.70	300	11.3
VECTor	0.6	Not available	10.00	Not available	Not available
MuPET	1.25	14	6.38	1100	12.0

Appendix B

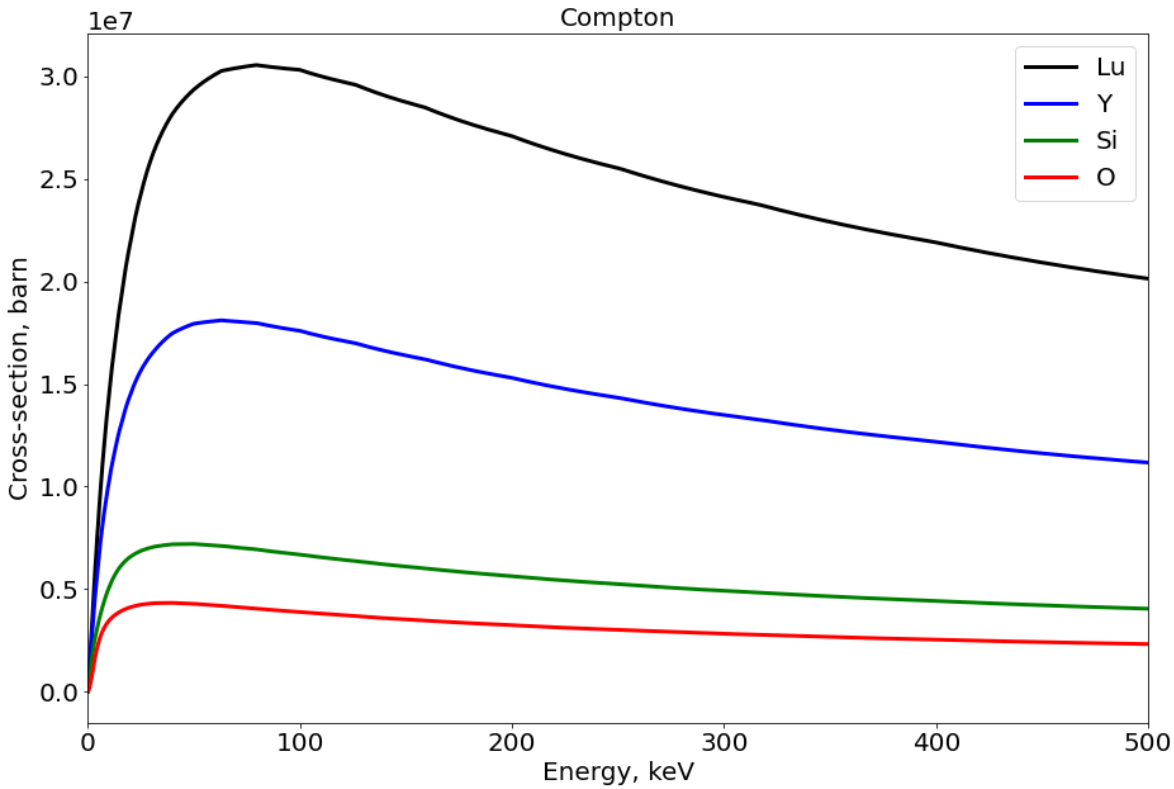

Figure B.1 – Compton scattering cross-sections for different LYSO's elements

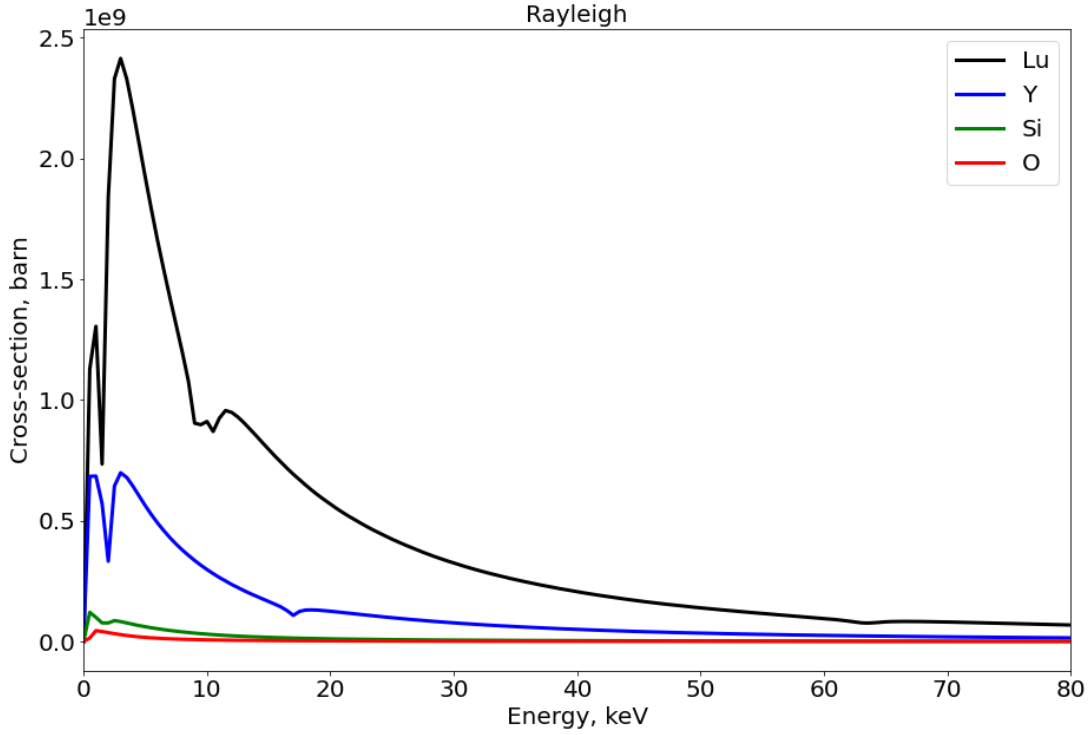

Figure B.2 – Rayleigh scattering cross-sections for different LYSO's elements

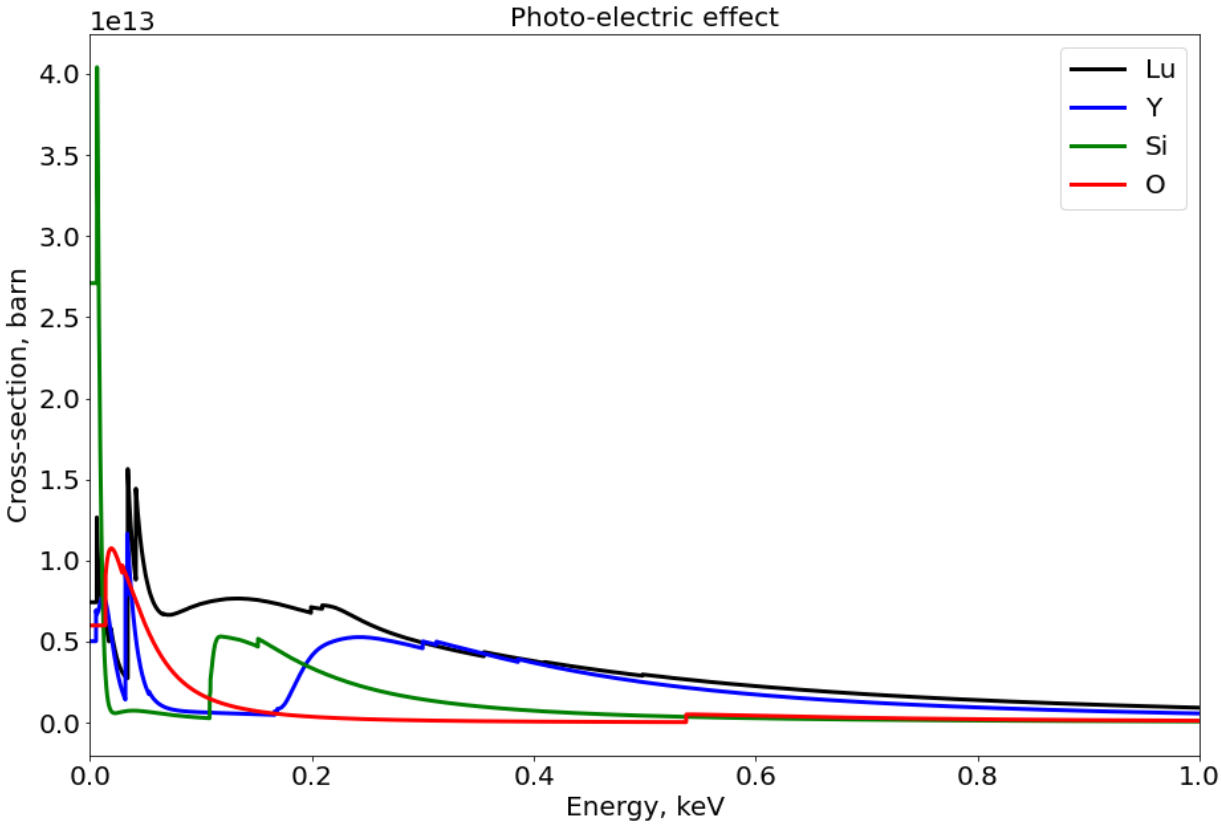

Figure B.3 – Photo-electric effect cross-sections for different LYSO's elements

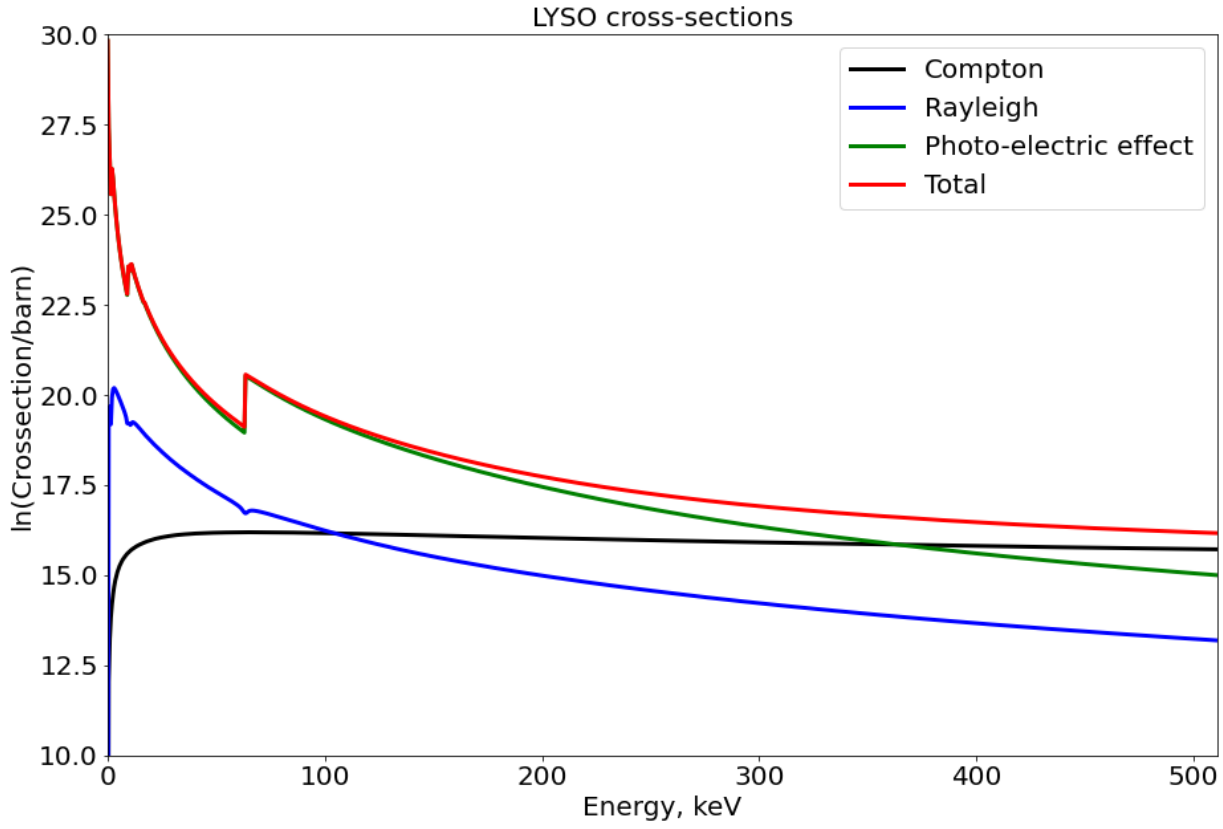

Figure B.4 – Overage LYSO cross-sections of different processes

Appendix C

Table C.1 – Optical properties of detector materials

Material	Density, g/cm^3	Refractive index	Light yield, photons/MeV	Decay time, ns	Absorption length, cm	Rayleigh attenuation lengths, cm
LYSO	7.1000	1.81	33200	36	50	260
Epoxy	1.2000	1.53	-	-	-	-
Air	0.0012	1.00	-	-	-	-

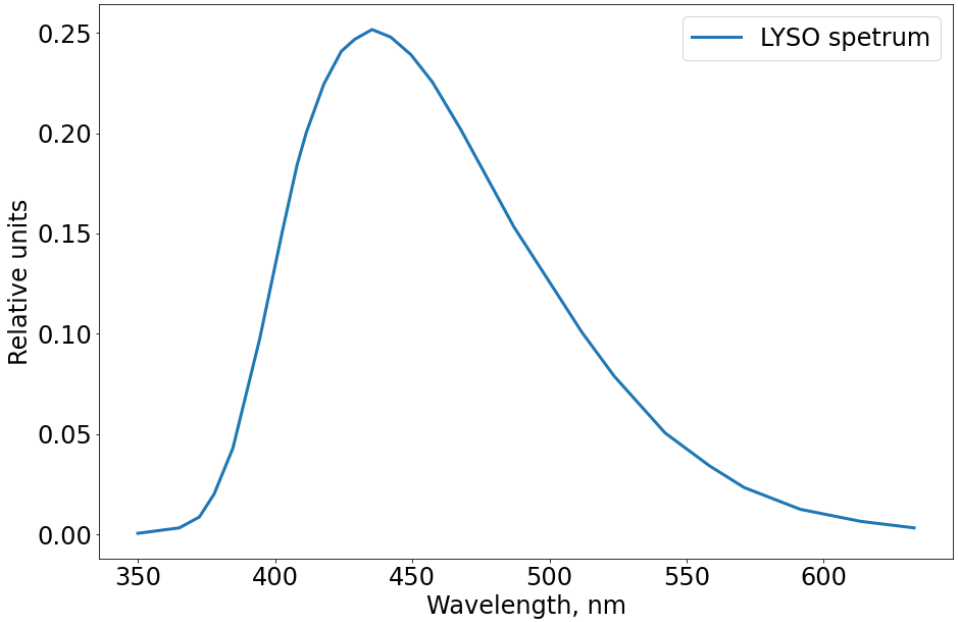

Figure C.2 – LYSO spectrum emission

Appendix D

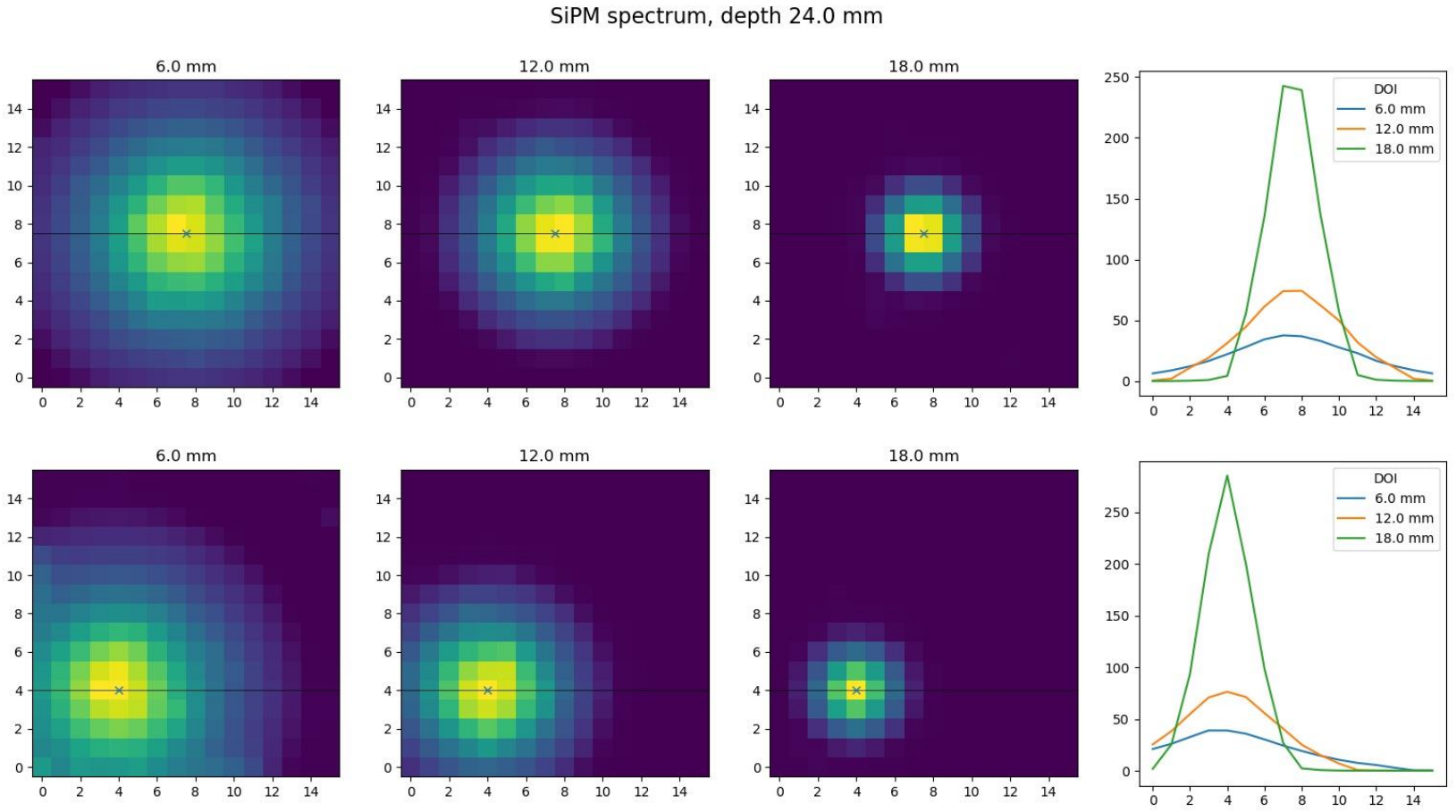

Figure D.1 – Distribution of counts on SiPM on different depths and source position

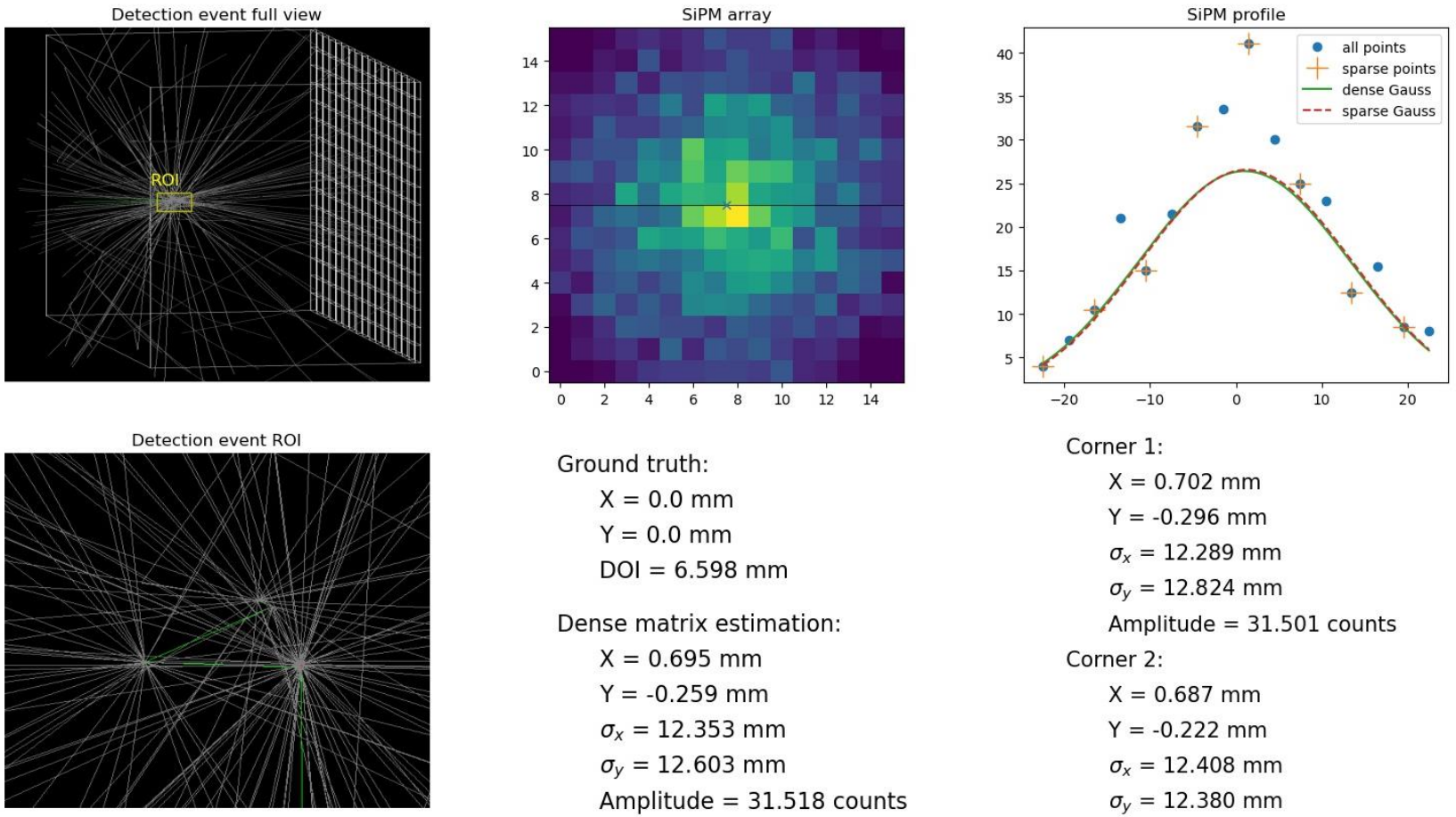

Figure D.2 – Example of near surface interaction of photon and SiPM's output with LYSO thickness 24 mm

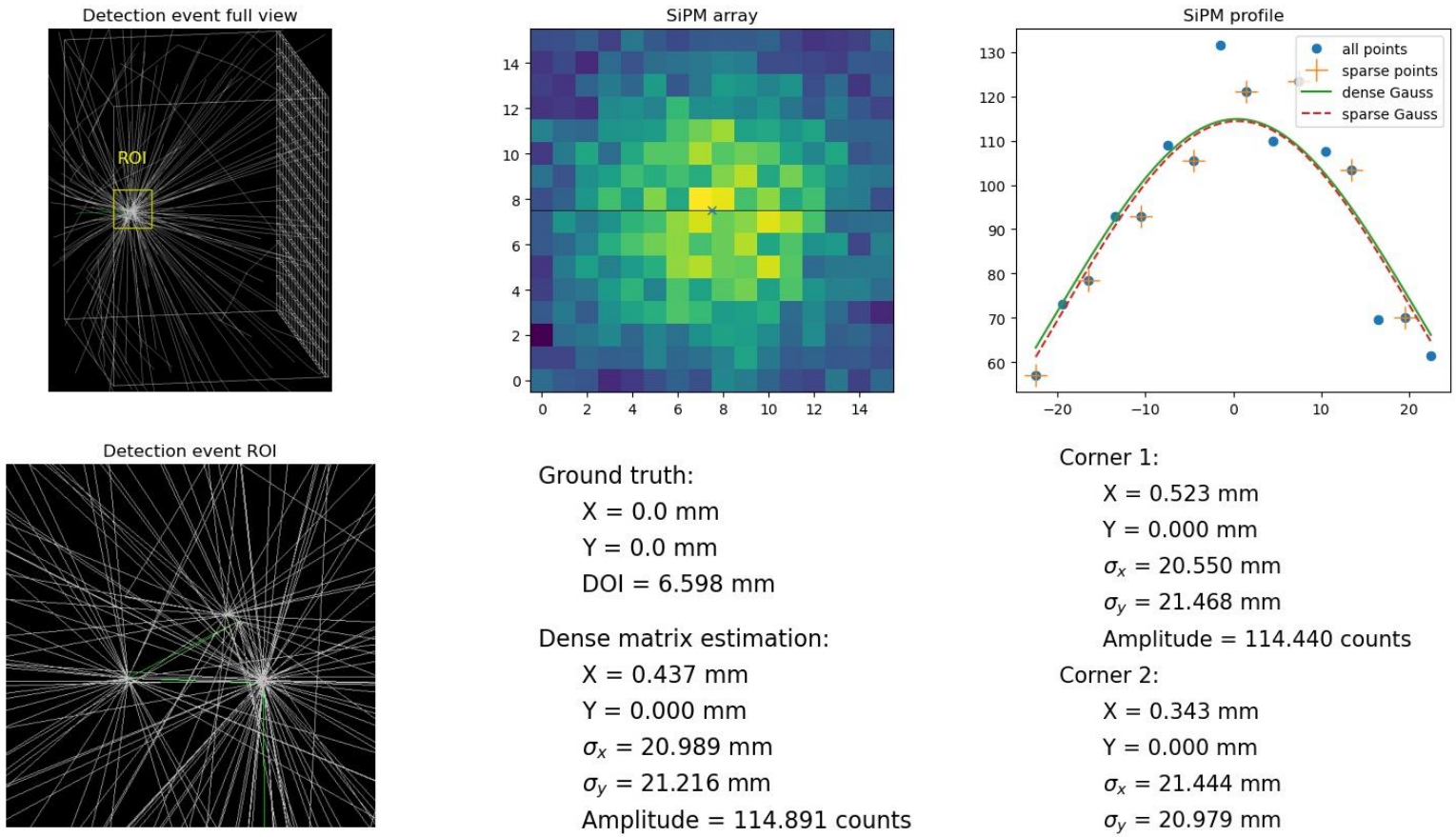

Figure D.3 – Example of near surface interaction of photon and SiPM's output with LYSO thickness 36 mm

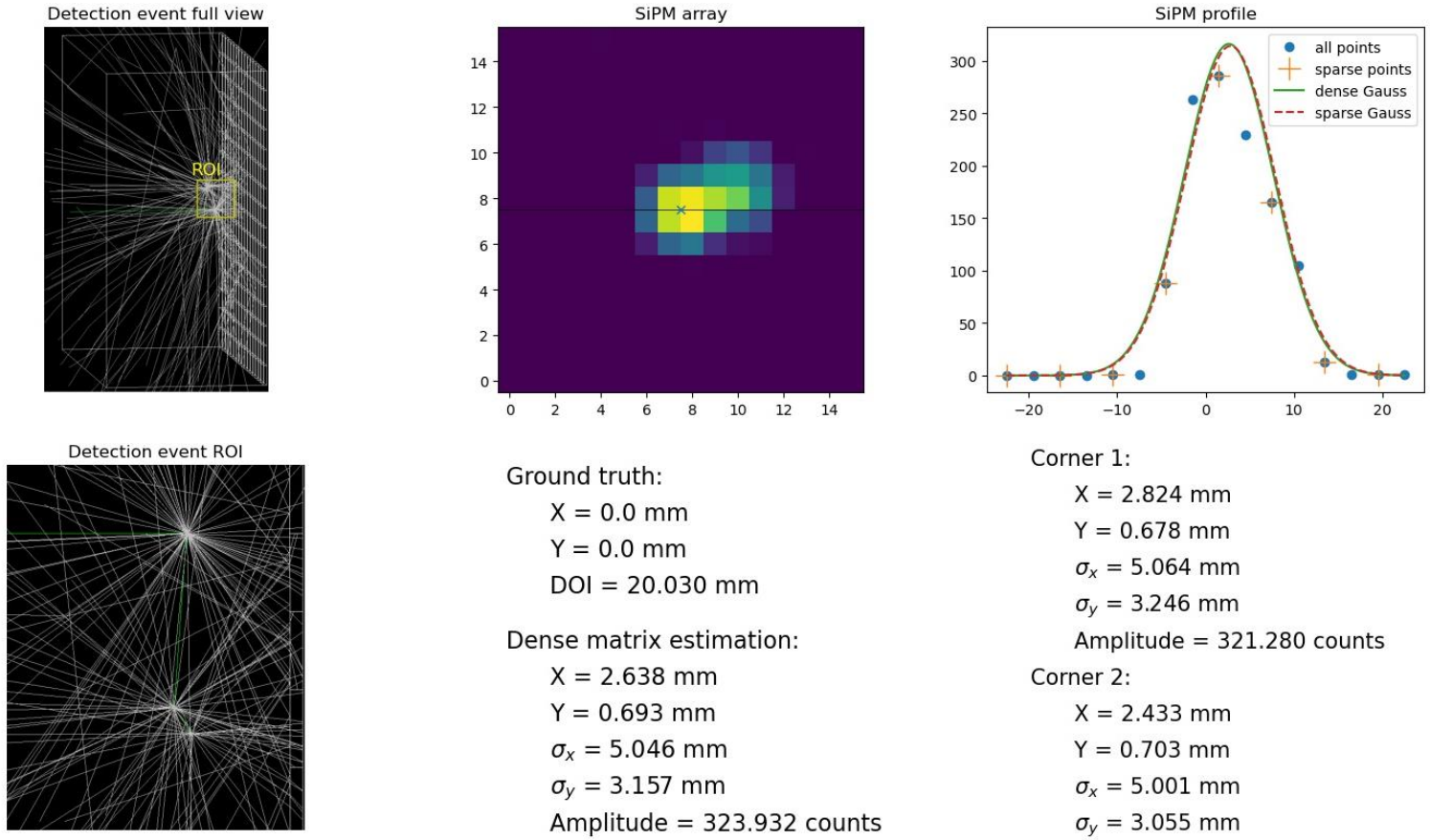

Figure D.4 – Example of deep interaction of photon and SiPM's output with LYSO thickness 24 mm

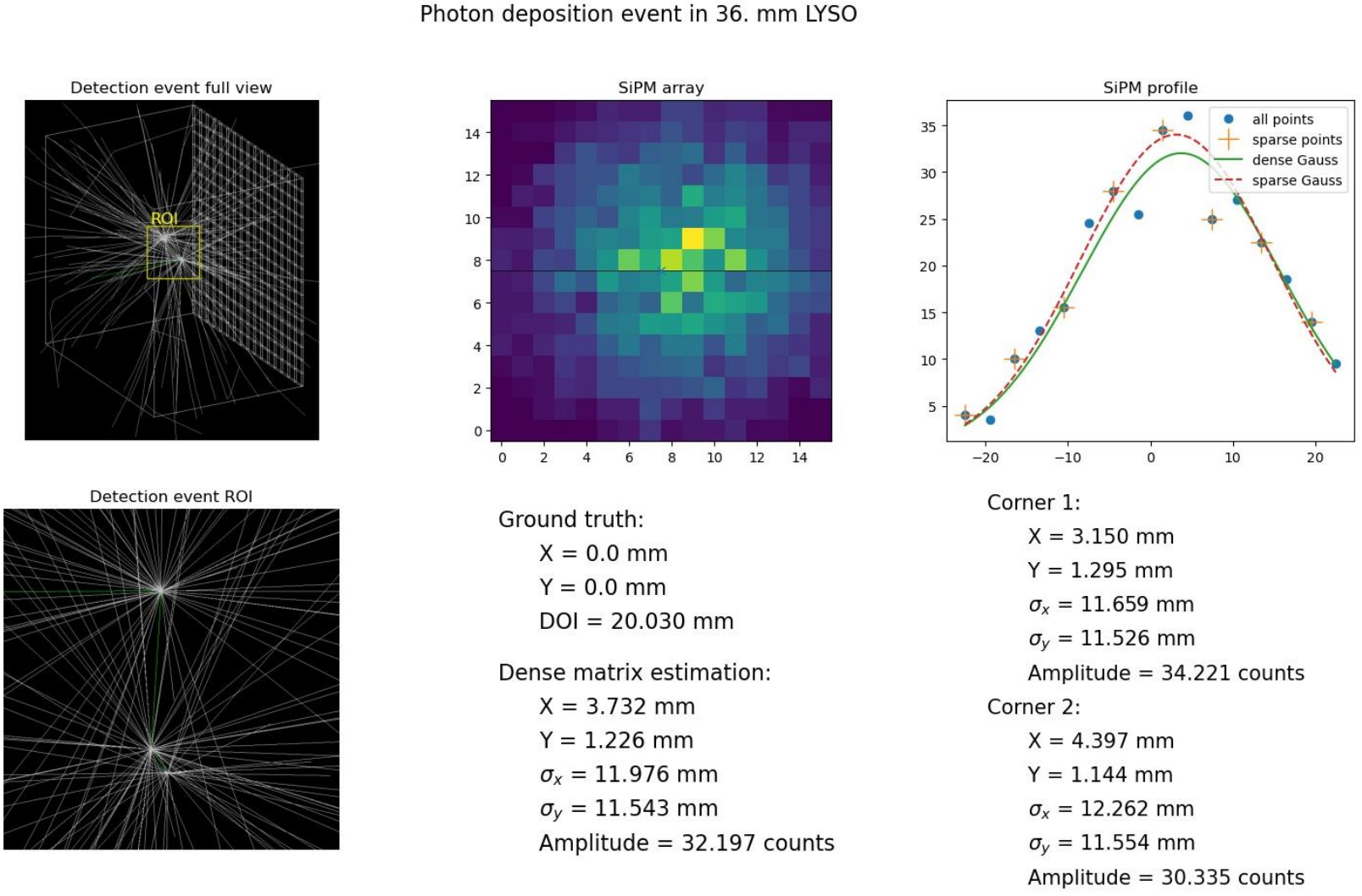

Figure D.5 – Example of deep interaction of photon and SiPM's output with LYSO thickness 36 mm